NASA TECHNICAL MEMORANDUM

NASA TM X-2712

NASA TM X-2712

LOW-SUBSONIC AERODYNAMIC CHARACTERISTICS OF A SHUTTLE-ORBITER CONFIGURATION DESIGNED FOR REDUCED LENGTH

by George M. Ware and Bernard Spencer, Jr.

Langley Research Center
Hampton, Va. 23365

NATIONAL AERONAUTICS AND SPACE ADMINISTRATION • WASHINGTON, D. C. • APRIL 1973

1. Report No.	2. Government Accession No.	3. Recipient's Catalog No.
NASA TM X-2712		

4. Title and Subtitle	5. Report Date
LOW-SUBSONIC AERODYNAMIC CHARACTERISTICS OF A SHUTTLE-ORBITER CONFIGURATION DESIGNED FOR REDUCED LENGTH	April 1973
	6. Performing Organization Code

7. Author(s)	8. Performing Organization Report No.
George M. Ware and Bernard Spencer, Jr.	L-8712
	10. Work Unit No. 502-37-01-01
9. Performing Organization Name and Address NASA Langley Research Center Hampton, Va. 23365	11. Contract or Grant No.
	13. Type of Report and Period Covered Technical Note
12. Sponsoring Agency Name and Address National Aeronautics and Space Administration Washington, D.C. 20546	14. Sponsoring Agency Code

15. Supplementary Notes

16. Abstract

An investigation has been made in the Langley low-turbulence pressure tunnel to determine the low-subsonic aerodynamic characteristics of a 0.01875-scale model of a potential shuttle orbiter. The design had the rocket engines mounted in fairings on either side of the body on top of the wing. The wing had a leading-edge sweep of 50° and a trailing-edge sweep of -4°. Configurations investigated included engine-mounted twin dorsal tails at various roll-out angles, a body-mounted center-line vertical tail, cylindrical and boattailed afterbody, and elevon and rudder at several deflections.

17. Key Words (Suggested by Author(s))	18. Distribution Statement
Shuttle-orbiter Aerodynamics	Unclassified – Unlimited

19. Security Classif. (of this report)	20. Security Classif. (of this page)	21. No. of Pages	22. Price*
Unclassified	Unclassified	38	$3.00

*For sale by the National Technical Information Service, Springfield, Virginia 22151

LOW-SUBSONIC AERODYNAMIC CHARACTERISTICS OF A SHUTTLE-ORBITER CONFIGURATION DESIGNED FOR REDUCED LENGTH

By George M. Ware and Bernard Spencer, Jr.
Langley Research Center

SUMMARY

An investigation has been conducted in the Langley low-turbulence pressure tunnel to determine the low-subsonic aerodynamic characteristics of a 0.01875-scale model of a "split-engine" shuttle-orbiter configuration. Tests were made at Mach numbers less than 0.30 over an angle-of-attack range from about -2° to 22° at 0° and 6° of sideslip. Most of the investigation was made at a Reynolds number of 13.9×10^6 based on body length. Configuration variations included either center or twin tails and cylindrical or boattailed body as well as deflected longitudinal, lateral, and directional control surfaces.

The results of the investigation indicated that boattailing the aft body increased the maximum lift-drag ratio by about 1.1 to a value of 7.75 for the twin-tail case but gave more negative (out of trim) values of pitching moment. The cylindrical-body configuration with a center tail had a maximum trimmed lift-drag value of 7.0 with an elevon deflection of 0°. In general, all configurations were slightly unstable longitudinally at the lower angles of attack and had low values of stability at the higher angles of attack about the center-of-gravity location of the present study (0.651 body length). All configurations were directionally stable and had positive effective dihedral.

INTRODUCTION

The National Aeronautics and Space Administration and the aerospace industry are currently investigating, both experimentally and analytically, a space shuttle system suitable for transportation of large payloads to and from near-earth orbit. Typically the orbiters under current study (ref. 1) have the main propulsion system located aft of the cargo bay. In examining potential means of reducing vehicle size, Langley Research Center has investigated a concept for which the engines were relocated in fairings on top of the wing alongside the body (cargo bay). The resulting configuration, therefore, was considerably different from previous orbiters.

The objective of the present study was to determine the effects of configuration variations on the low-subsonic aerodynamic characteristics of a 0.01875-scale model of the aforementioned "split-engine" orbiter. The tests were made in the Langley low-turbulence pressure tunnel at a Mach number of less than 0.30 over an angle-of-attack range from about -2° to 22° at 0° and 6° of sideslip. Most of the tests were conducted at a Reynolds number of 13.9×10^6 based on body length. Configurations investigated included either twin dorsal tails at various roll-out angles mounted on the engine fairings or a center-line vertical tail, a cylindrical afterbody, and boattailed afterbody.

SYMBOLS

The longitudinal characteristics are presented about the stability axes, and the lateral characteristics are presented about the body axes. All coefficients are normalized with respect to wing-planform area, extended to the body center line, and wing mean aerodynamic chord or wing span as defined in figure 1 and table I. The moment reference corresponded to 65.11 percent of the body length (29.44 percent mean aerodynamic chord), which was estimated to be the center-of-gravity location at landing without payload.

b reference span (maximum wing span), m

$\bar{c}$ mean aerodynamic chord of wing, m

C_D drag coefficient, $\frac{\text{Drag}}{q_\infty S}$

C_L lift coefficient, $\frac{\text{Lift}}{q_\infty S}$

C_l rolling-moment coefficient, $\frac{\text{Rolling moment}}{q_\infty S b}$

$C_{l_\beta} = \frac{\Delta C_l}{\Delta \beta}$, per deg, $\beta = 0^{\circ}$ and 6°

$C_{l_{\delta_a}}$ rolling-moment coefficient due to aileron deflection, $\frac{\Delta C_l}{\Delta \delta_a}$, per deg

$C_{l_{\delta_r}}$ rolling-moment coefficient due to rudder deflection, $\frac{\Delta C_l}{\Delta \delta_r}$, per deg

C_m pitching-moment coefficient, $\frac{\text{Pitching moment}}{q_\infty S\bar{c}}$

$C_{m,o}$ pitching-moment coefficient at zero lift

C_n yawing-moment coefficient, $\frac{\text{Yawing moment}}{q_\infty Sb}$

$C_{n_\beta} = \frac{\Delta C_n}{\Delta\beta}$, per deg, $\beta = 0^o$ and 6^o

$C_{n_{\delta_a}}$ yawing-moment coefficient due to aileron deflection, $\frac{\Delta C_n}{\Delta\delta_a}$, per deg

$C_{n_{\delta_r}}$ yawing-moment coefficient due to rudder deflection, $\frac{\Delta C_n}{\Delta\delta_r}$, per deg

C_Y side-force coefficient, $\frac{\text{Side force}}{q_\infty S}$

$C_{Y_\beta} = \frac{\Delta C_Y}{\Delta\beta}$, per deg, $\beta = 0^o$ and 6^o

$C_{Y_{\delta_a}}$ side-force coefficient due to aileron deflection, $\frac{\Delta C_Y}{\Delta\delta_a}$, per deg

$C_{Y_{\delta_r}}$ side-force coefficient due to rudder deflection, $\frac{\Delta C_Y}{\Delta\delta_r}$, per deg

L/D lift-drag ratio

q_∞ free-stream dynamic pressure, N/m^2

R Reynolds number based on body length

S projected wing-planform area, m^2

α angle of attack, deg

β angle of sideslip, deg

δ_a aileron deflection angle, $\frac{\delta_{e,L} - \delta_{e,R}}{2}$ (positive for right-roll command), deg

δ_e elevon deflection angle measured normal to hinge line (positive when trailing edge deflected down), deg

δ_r rudder deflection angle, $\frac{\delta_{r,L} + \delta_{r,R}}{2}$, measured normal to hinge line (positive for trailing edge left, viewed from rear), deg

ϕ twin-tail roll-out angle (measured from vertical), deg

Subscripts:

L left

max maximum

R right

TESTS AND CORRECTIONS

The tests were made in the Langley low-turbulence pressure tunnel at Reynolds numbers, based on body length, ranging from 13.9×10^6 to 20.9×10^6, with the major portion of the tests made at 13.9×10^6 at Mach numbers less than 0.30. The angle of attack was varied from about -2° to 22° at 0° and 6° of sideslip.

The model was sting supported and forces and moments were measured with a six-component strain-gage balance. The balance and sting were calibrated for the effects of bending under load in both the longitudinal and lateral planes. In all cases the drag presented herein represents gross drag since base drag is included. Standard wind-tunnel corrections for the effects of tunnel blockage and jet boundary have been applied to the data by the methods described in references 2 and 3.

DESCRIPTION OF MODEL

Sketches and photographs of the 0.01875-scale model are presented in figures 1 and 2, respectively. The wing had an aspect ratio of 2.4 with a 50° leading-edge sweep and a -4° trailing-edge sweep. Engines were mounted in fairings above the wing and alongside the body. The body was tested with both a cylindrical aft section and a boattailed aft section.

Two dorsal tail configurations were investigated: a body-mounted center tail and a set of twin tails mounted on the engine fairings alined with the model center line. The

twin tails were tested at roll-out angles, measured from the vertical, of 0^{o}, 15^{o}, and 30^{o}. For control surfaces, the model had elevons in the wing trailing edge which extended from the engine fairings to the wing tips, rudders in both the center and twin tails, and a body-mounted base flap which was fixed at 0^{o} for this investigation. A more detailed description of model geometry is presented in table I.

RESULTS AND DISCUSSION

Longitudinal Aerodynamic Characteristics

Effect of Reynolds number.- The effect of increasing Reynolds number on the longitudinal aerodynamic characteristics of the model is presented in figure 3. The boattailed body with twin tails was selected for these tests as it was considered the configuration most sensitive to changes in Reynolds number. The data show that increasing Reynolds number had no effect on lift-curve slope or stability level at angles of attack below about 15^{o} and produced only minor changes in these parameters at higher angles of attack. There were, in general, reductions in drag at lift coefficients greater than about 0.35 which are reflected in higher values of maximum lift-drag ratio with increasing Reynolds number. It appears, also, that drag due to lift had not become constant for the test Reynolds number range. Because of the preliminary nature of the design and the number of configuration variables, it was decided, however, to expedite testing by conducting the remainder of the tests at a Reynolds number of 13.9×10^{6} recognizing that values of $(L/D)_{max}$ may be conservative.

Effect of boattail and various tail configurations.- The effect of various configuration components on the longitudinal characteristics of the model is presented in figure 4. Comparison of the data for the boattail afterbody model and the cylindrical afterbody model with tails off indicates that the boattailed configuration produced considerably more lift and less drag than the cylindrical-afterbody configuration. The addition of the twin tails, acting as end plates, increased the effectiveness of the boattail giving higher values of lift and lift-curve slope. The maximum lift-drag values varied from about 7.75 for the boattail-body twin-tail configuration to about 6.65 for the cylindrical-body twin-tail configuration. The cylindrical-body center-tail configuration had an $(L/D)_{max}$ of about 7.0.

With the center-of-gravity location of the present investigation (0.651 body length) all configurations were slightly unstable at angles of attack below that for $(L/D)_{max}$ and had low values of stability at the higher angles of attack. The cylindrical-body configuration with either twin or center tails was trimmed $(\delta_e = 0^{o})$ with neutral longitudinal stability from angles of attack of about 7^{o} to 11^{o} which included the angles of attack for maximum lift-drag ratio.

The boattailed twin-tail configuration, with large negative pressures over the aft portion of the body, had negative $C_{m,o}$ and negative values of pitching moments over

the angle-of-attack range with no longitudinal trim for zero elevon deflection. It is interesting to note that negative $C_{m,o}$ resulted from the addition of the center vertical tail to the cylindrical-body model. Usually adding a drag-producing area above the center of gravity results in a positive increment in pitching moment. In the present case, however, the flow expanding around the rather thick (12 percent of the chord, see table I) center tail apparently reduced the pressure over the aft body creating additional lift and an increment of nose-down moment. This assumption can be substantiated partially by noting the slightly higher values of lift for the tail-on configuration. The same results have been noted from unpublished data on an identical airfoil tail added to a configuration having a similarly wide base.

Effect of twin-tail roll-out angle.- Rotating the twin tails from 0^o to 15^o and 30^o from the vertical (see fig. 5) added lift aft of the center of gravity which resulted in low-lift stability changes from $-0.006\bar{c}$ to $0.014\bar{c}$ and $0.034\bar{c}$, respectively. Untrimmed maximum lift-drag ratios were also increased from 6.65 for $\phi = 0^o$ to 6.75 for $\phi = 15^o$ and 6.95 for $\phi = 30^o$.

Effect of elevon deflection.- Data for elevon deflection with the cylindrical-body configuration having twin- or center-tail arrangements are shown in figures 6(a) and 6(b), respectively. For the twin-tail configuration (fig. 6(a)), negative elevon deflection caused a slight increase in lift-curve slope and an accompanying increase in longitudinal stability. This effect on stability is somewhat unusual in subsonic incompressible flow and is not present for the configuration with the center vertical tail (fig. 6(b)). It appears that when the elevons were deflected, a change in local stream angle occurred which affected the rolled-out twin tails, thereby increasing tail lift and resulting in an overall stabilizing effect.

Lateral-Directional Aerodynamic Characteristics

Effect of various tail configurations.- The lateral-directional stability characteristics are presented as the variation of the stability derivatives C_{Y_β}, C_{n_β}, and C_{l_β} with angle of attack in figures 7 and 8. These parameters were obtained by taking the difference in lateral coefficients measured at angles of sideslip of 0^o and 6^o over the test angle-of-attack range and therefore do not account for any nonlinearities which may occur in the intermediate β-range.

The effect of various tail configurations was investigated with the cylindrical-body model only. The data show that the model was directionally stable and had positive effective dihedral $\left(-C_{l_\beta}\right)$ at positive angles of attack for all configurations. The center tail, although somewhat smaller than the total area of the twin tails, was more effective in

stabilizing the model. Rolling the twin tails from the vertical progressively decreased directional stability and increased the effective dihedral parameter. In addition, rolling the tails out tended to linearize C_{n_β} with α by effectively moving the tail out of the influence of vorticity produced at the wing-body juncture. The effect of boattailing the aft body for the body-wing combinations without tails (see fig. 8) shows that there was a loss in directional stability and an increase in positive effective dihedral resulting from the loss in side area at the rear of the model.

Lateral-directional control characteristics.- The effect of rudder deflection as a yaw control and aileron (differential elevon) deflection as a roll control for the cylindrical body model with center and twin tails is presented in figures 9 and 10, respectively.

Comparison of the rudder effectiveness $C_{n_{\delta_r}}$ for center and twin tails shows that the twin tails, even though they were rolled out to 15°, were more effective than the center tail as a yaw control. This result should be tempered by the fact that the rudder area was greater for the twin-tail configuration (see table I). Rudder deflection on both tail arrangements caused adverse rolling moments.

The ailerons (fig. 10) were a more effective roll control when deflected in the presence of the center tail than in the presence of the twin tails. The reason for this is not obvious but is probably associated with flow interference between elevon and twin tail as was indicated in the longitudinal control characteristics of figure 6(a). Increasing the aileron deflection angle for the twin-tail model from 2.5° to 10° reduced the value of $C_{l_{\delta_a}}$ and had little effect on the unit yawing moment produced by aileron deflection. Aileron deflection produced favorable yawing moments for both tail configurations.

SUMMARY OF RESULTS

Low-subsonic wind-tunnel tests have been made to determine the static longitudinal and lateral aerodynamic characteristics of a shuttle-orbiter configuration designed for reduced length. The results of the investigation may be summarized as follows:

1. Boattailing the aft body increased the maximum lift-drag ratio of the model by about 1.10 from 6.65 for the cylindrical-body twin-tail configuration to 7.75 for the boattailed twin-tail configuration but also gave more negative (out of trim) values of pitching moment.

2. The cylindrical-body center-tail configuration had a maximum trimmed lift-drag value of 7.0 with an elevon deflection of 0°.

3. In general, all configurations were slightly unstable longitudinally at the lower angles of attack and had low values of stability at the higher angles of attack about the center-of-gravity location of the present investigation (0.651 body length).

4. All configurations were directionally stable and had positive effective dihedral.

Langley Research Center,
National Aeronautics and Space Administration,
Hampton, Va., February 1, 1973.

REFERENCES

1. Anon.: Space Shuttle Program, Phase B Final Report. Vol. II – Technical Summary, Book 2, Pt. 2. SD 71-114-2 (Contract NAS 9-10960), North American Rockwell Corp., June 25, 1971. (Available as NASA CR-119776.)

2. Swanson, Robert S.; and Toll, Thomas A.: Jet-Boundary Corrections for Reflection-Plane Models in Rectangular Wind Tunnels. NACA Rep. 770, 1943. (Supersedes NACA WR L-458.)

3. Herriot, John G.: Blockage Corrections for Three-Dimensional-Flow Closed-Throat Wind Tunnels, With Consideration of the Effect of Compressibility. NACA Rep. 995, 1950. (Supersedes NACA RM A7B28.)

TABLE I.- GEOMETRIC CHARACTERISTICS OF 0.01875-SCALE MODEL

Body:	
Overall length, cm (in.)	53.101 (20.906)
Maximum height, cm (in.)	10.620 (4.181)
Maximum width, cm (in.)	20.320 (8.000)
Wing:	
Root chord at body center line, cm (in.)	34.996 (13.778)
Tip chord, cm (in.)	4.991 (1.965)
*M.A.C., cm (in.)	23.937 (9.424)
*Span, cm (in.)	48.577 (19.125)
*Total planform area, m^2 (ft^2)	0.098 (1.056)
Elevon total planform area, m^2 (ft^2)	0.014 (0.150)
Leading-edge sweep, deg	50
Trailing-edge sweep, deg	4
Dihedral, deg	7
Incidence at body, deg	2
Incidence at tip, deg	-3
Airfoil section at root	NACA 0008-64
Airfoil section at tip	NACA 0012-64
Aspect ratio	2.4
Twin tails (each): [a]	
Root chord, cm (in.)	12.382 (4.875)
Tip chord, cm (in.)	3.810 (1.500)
Span, cm (in.)	12.090 (4.760)
Area, cm^2 (in^2)	97.890 (15.173)
Area, rudder, cm^2 (in^2)	39.071 (6.056)
Leading-edge sweep, deg	45
Trailing-edge sweep, deg	16
Airfoil section	NACA 0010-64
Aspect ratio	1.487
Center tail: [a]	
Root chord, cm (in.)	13.716 (5.400)
Tip chord, cm (in.)	6.350 (2.500)
Span, cm (in.)	13.970 (5.500)
Area, cm^2 (in^2)	55.182 (21.725)
Area, rudder, cm^2 (in^2)	22.073 (8.690)
Leading-edge sweep, deg	45
Trailing-edge sweep, deg	25
Airfoil section	NACA 0012-64
Aspect ratio	1.392

*Model reference dimensions.

[a] Theoretical values measured at or from a line parallel to the model center line passing through the juncture of the rudder hinge line and the body. The dimensions include cutout areas of the rudder.

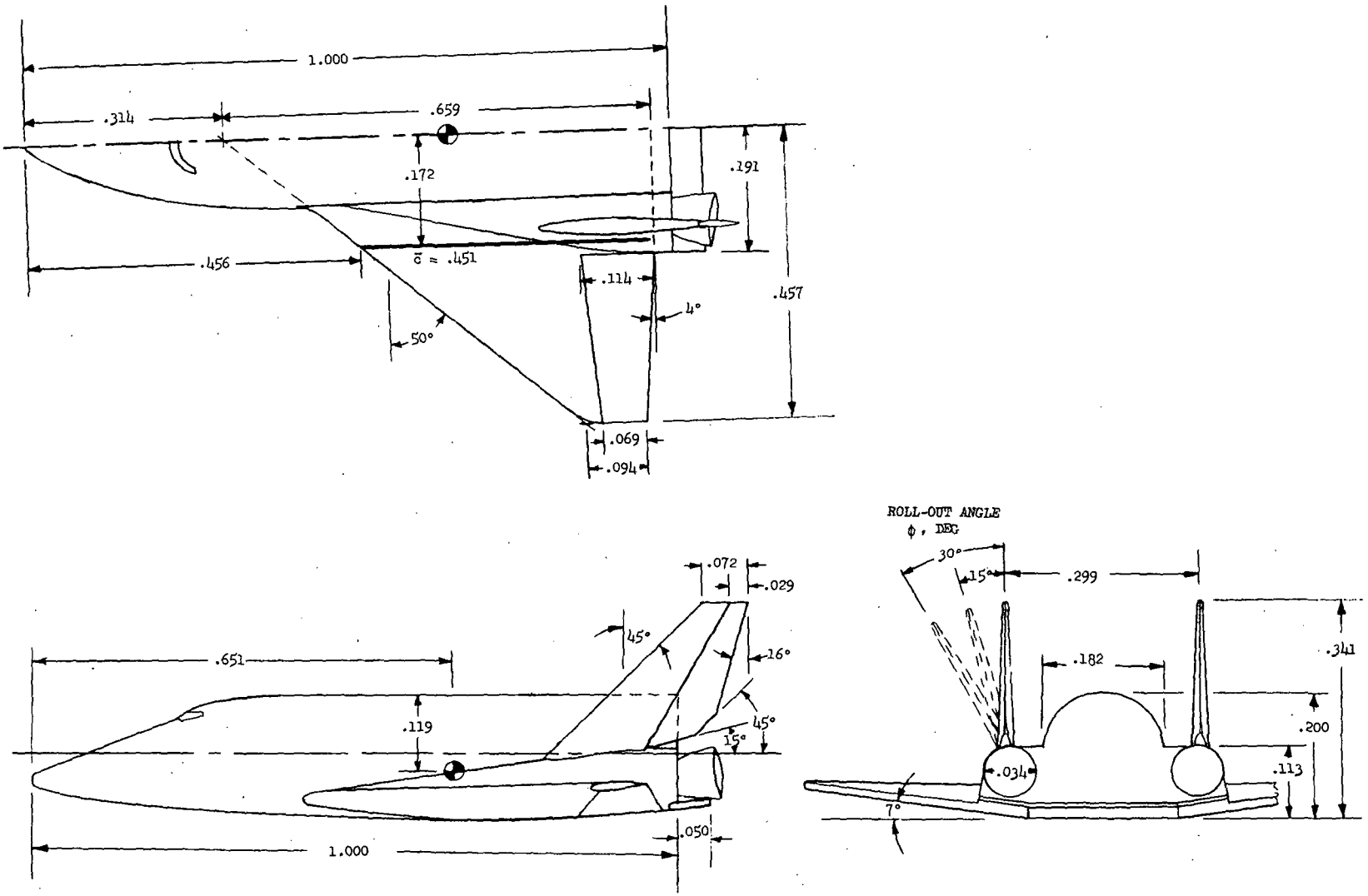

(a) Cylindrical body, twin-tail configuration.

Figure 1.- Sketches of model used in investigation. All dimensions normalized to body length. Body length = 53.101 cm (20.906 in.).

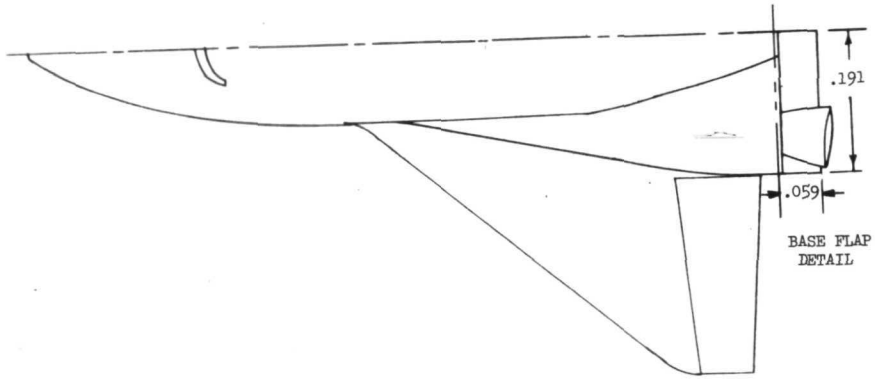

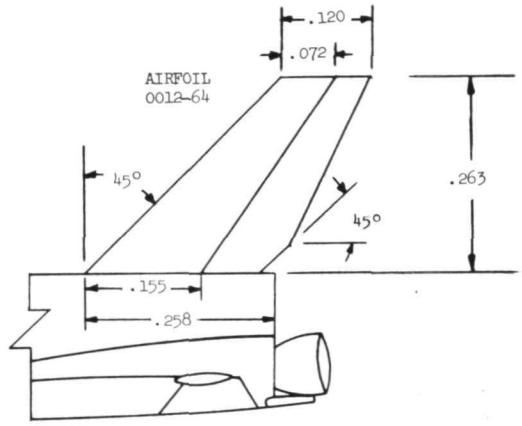

CENTER VERTICAL TAIL DETAIL
(CYLINDRICAL BODY ONLY)

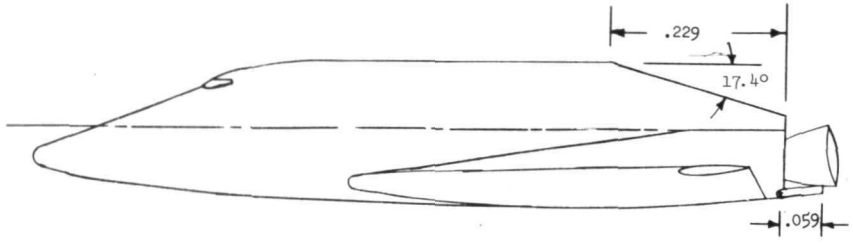

BOATTAIL BODY DETAIL

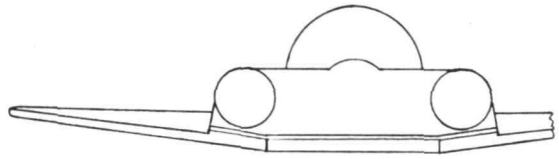

(b) Boattail body and cylindrical body with center tail.

Figure 1.- Concluded.

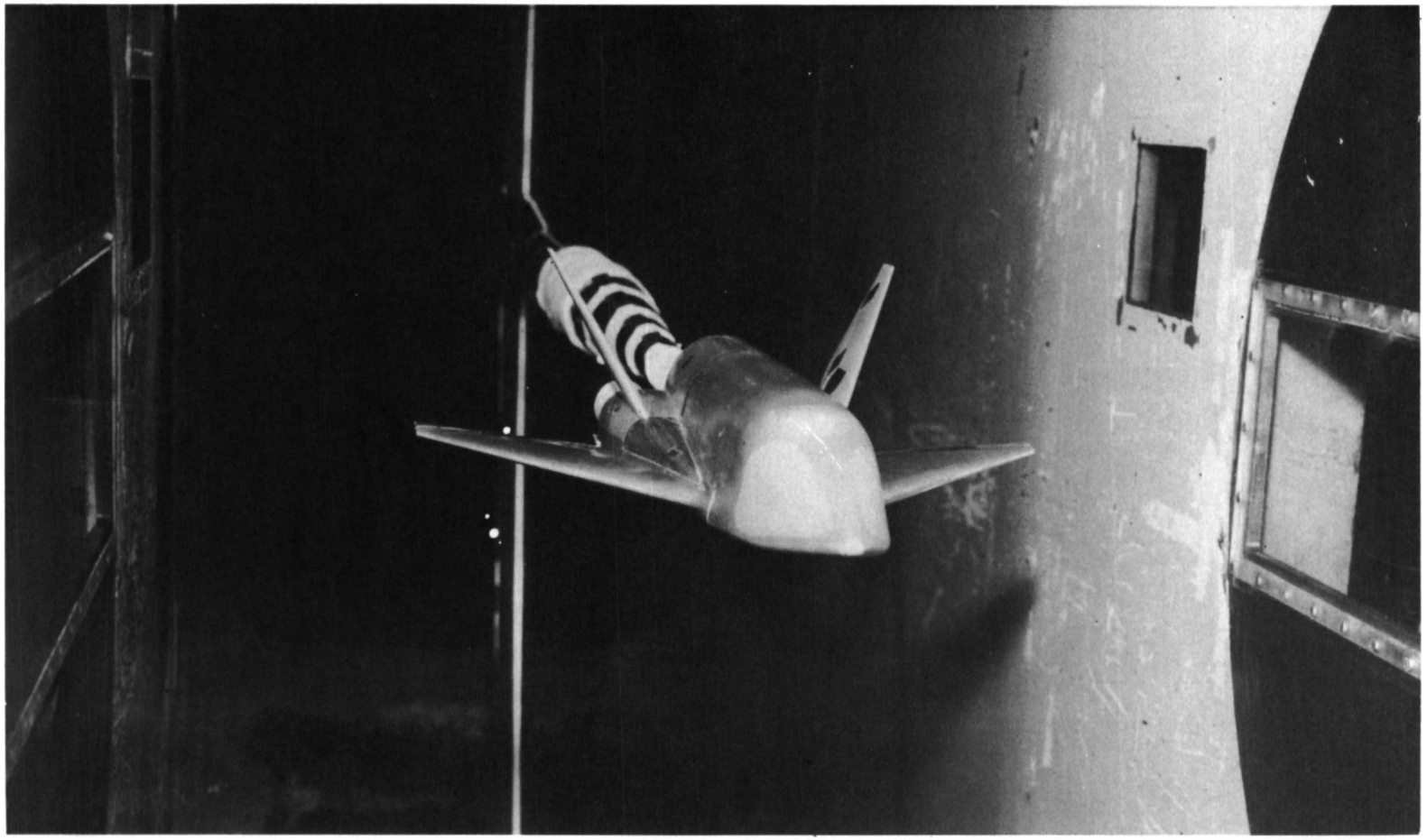

L-72-4700

(a) Three-quarter front view from above.

Figure 2.- Photographs of model mounted in Langley low-turbulence pressure tunnel.

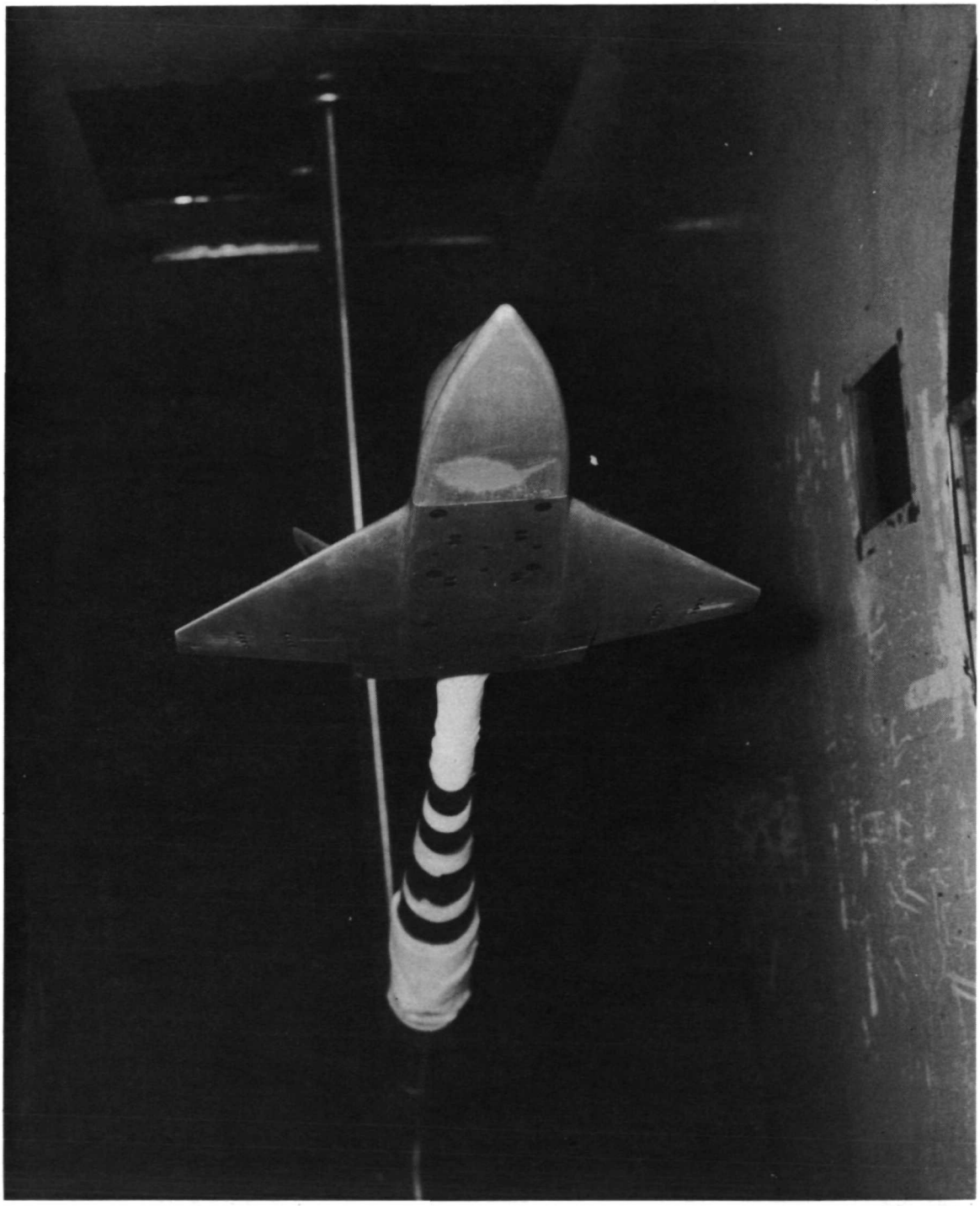

L-72-4701

(b) Three-quarter front view from below.

Figure 2.- Continued.

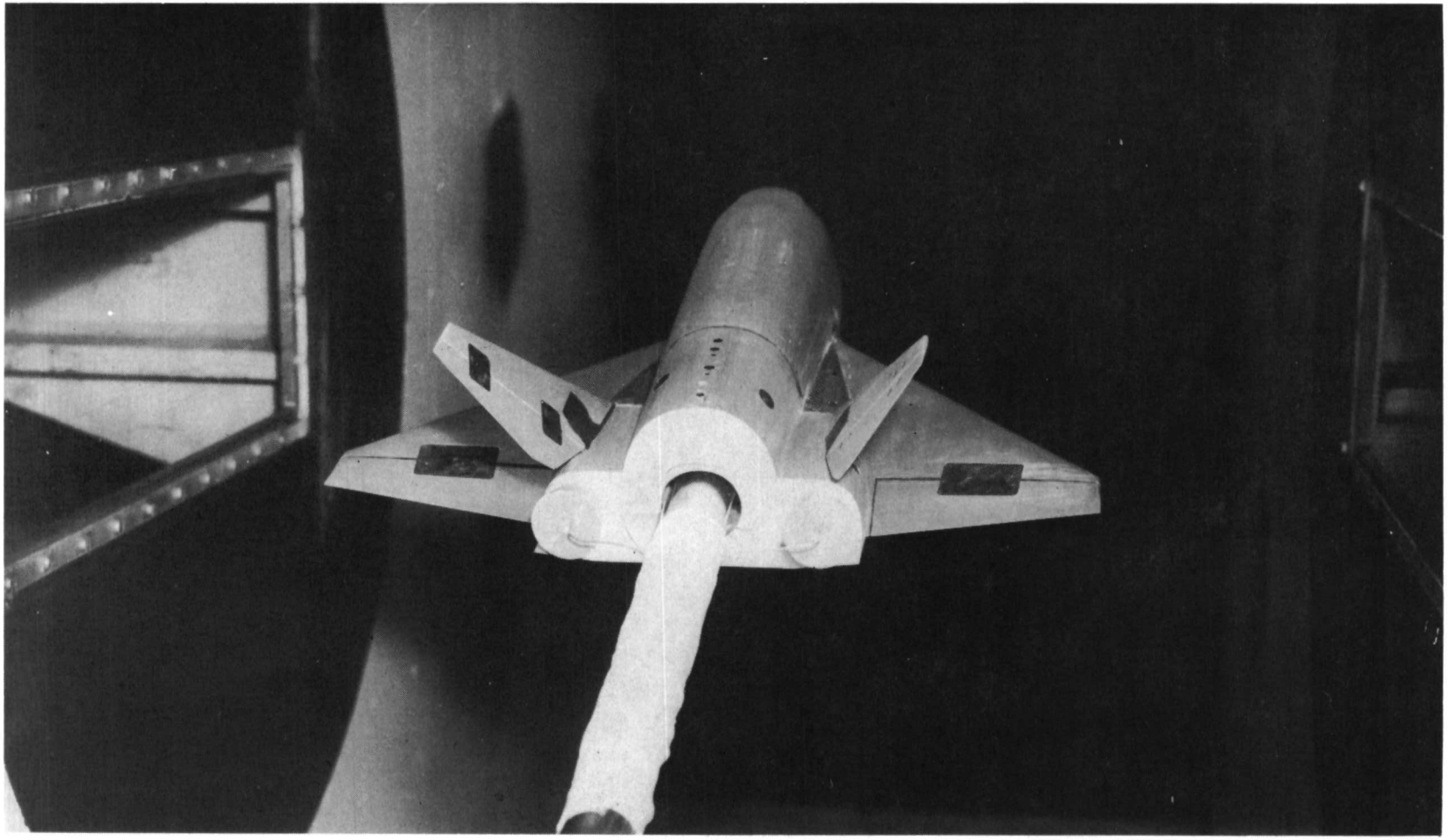

L-72-4699

(c) Rear view.

Figure 2.- Concluded.

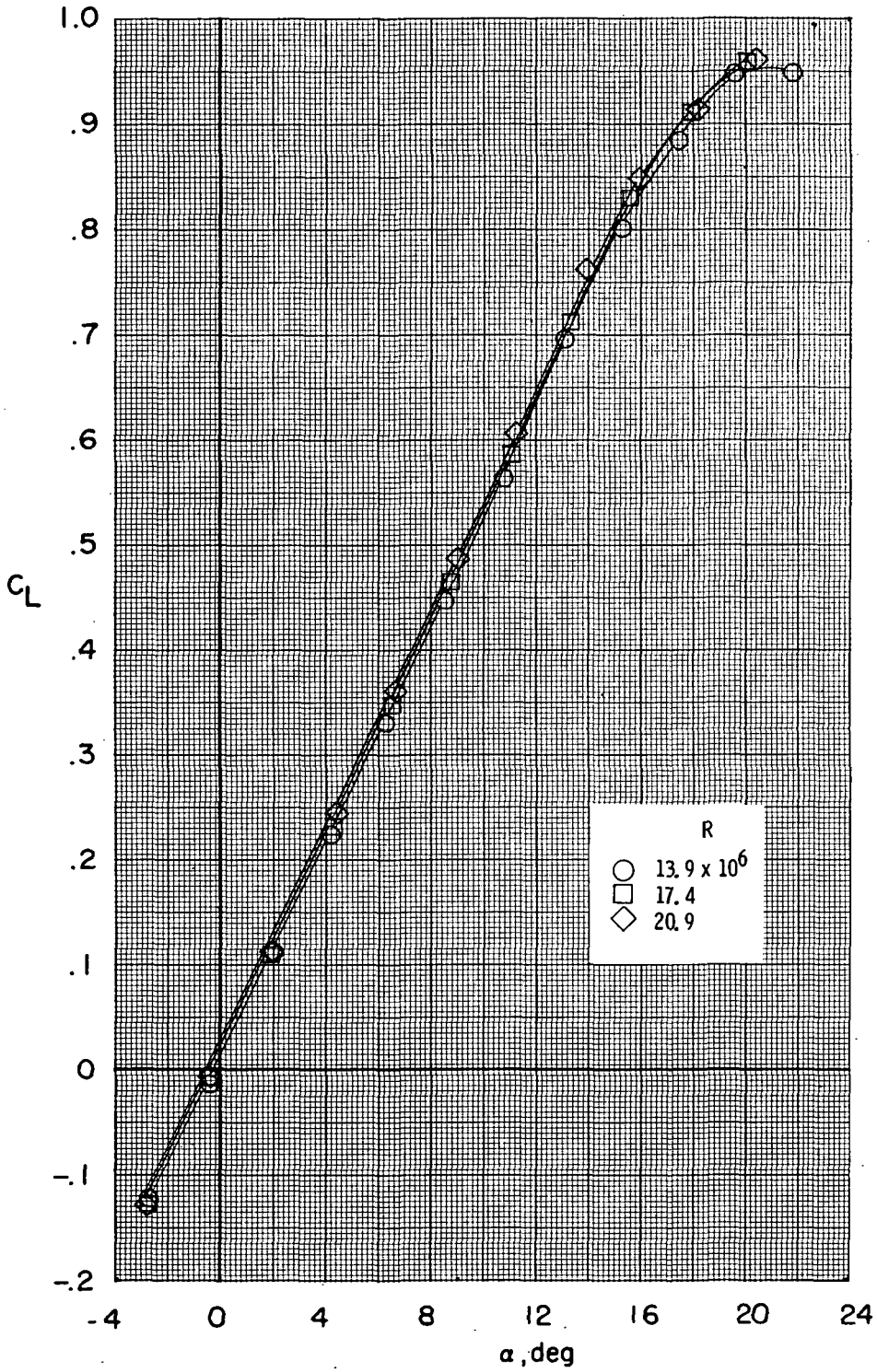

Figure 3.- Effect of Reynolds number on longitudinal aerodynamic characteristics of model. Boattail body; twin tails ($\phi = 15^{o}$); $\delta_e = 0^{o}$; $\beta = 0^{o}$.

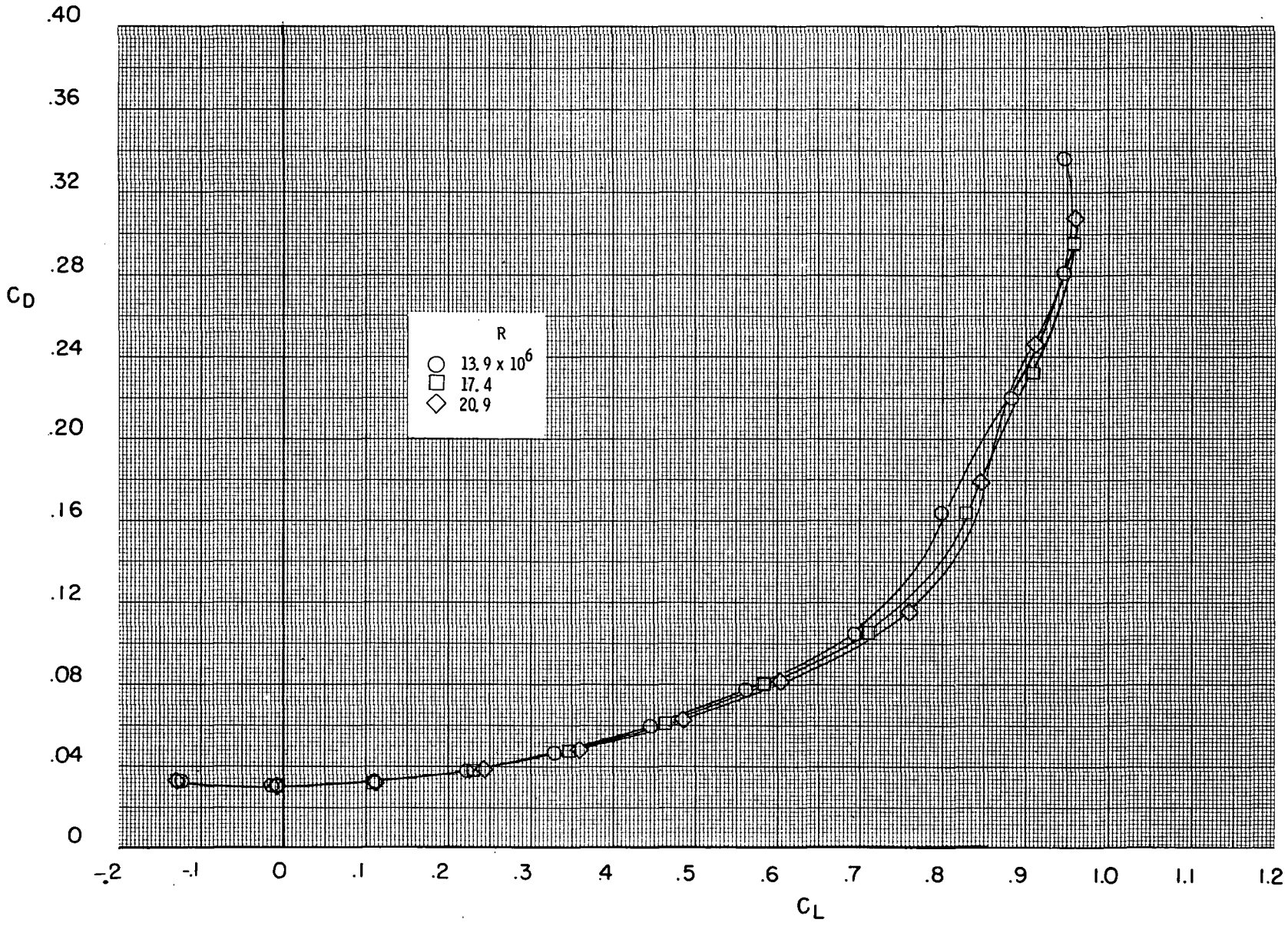

Figure 3.- Continued.

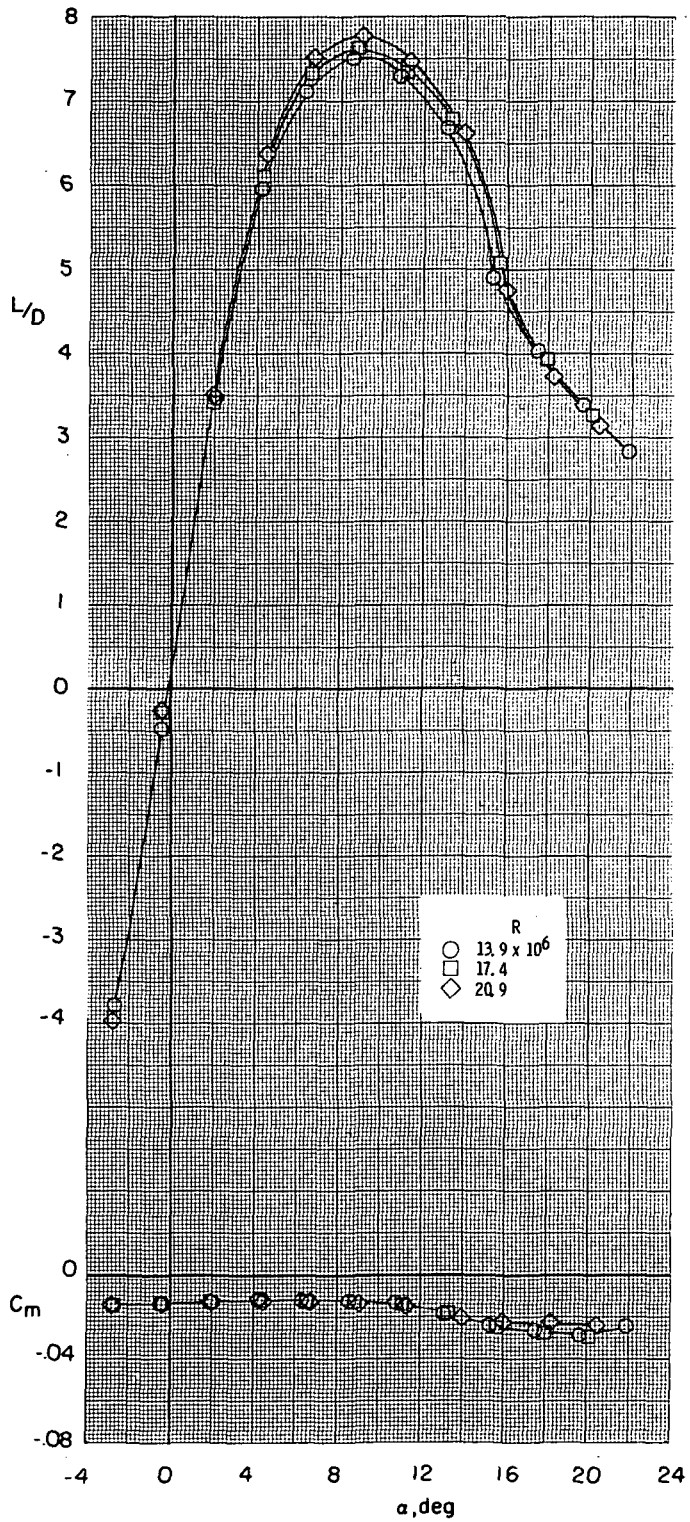

Figure 3.- Continued.

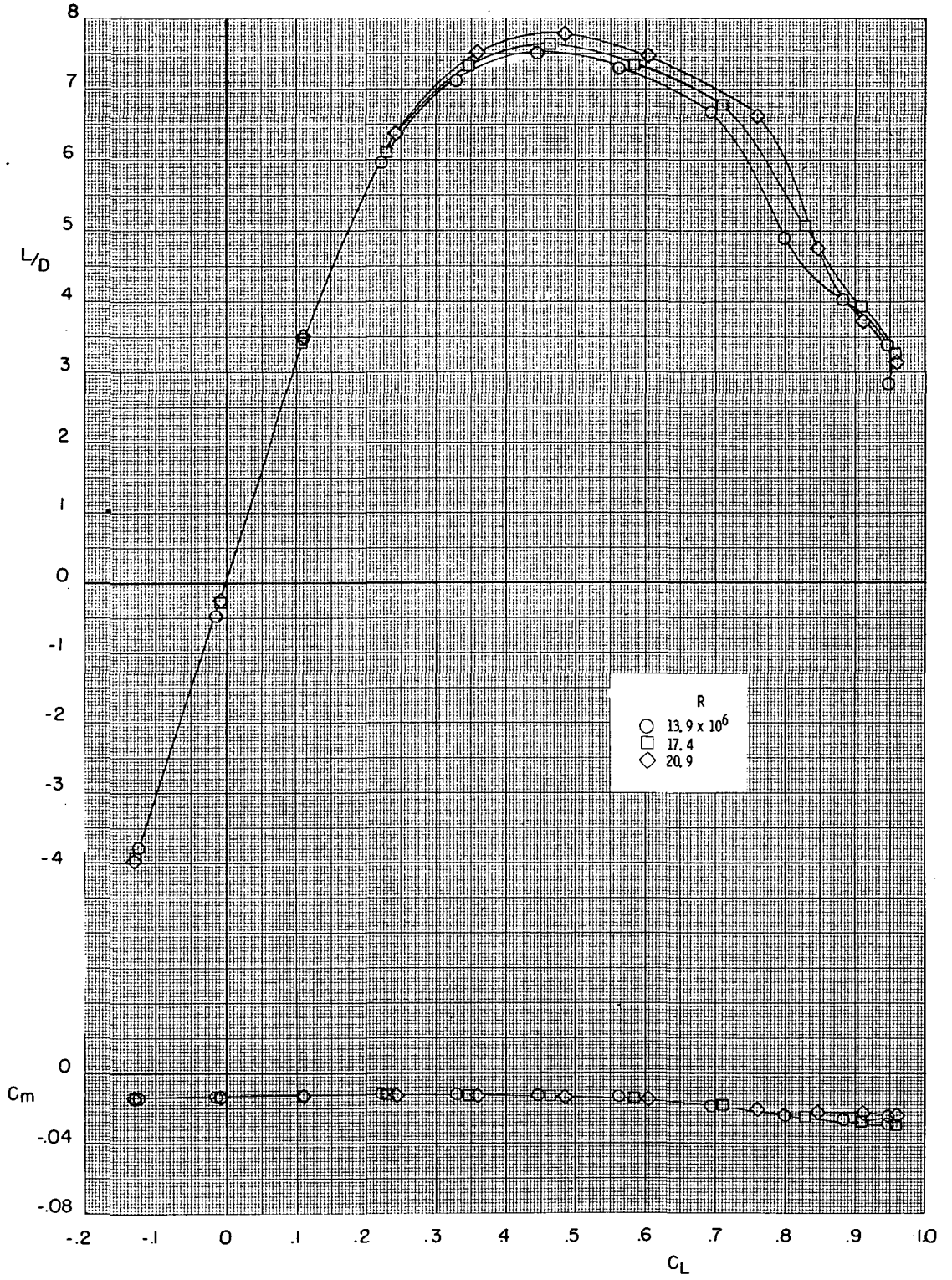

Figure 3.- Concluded.

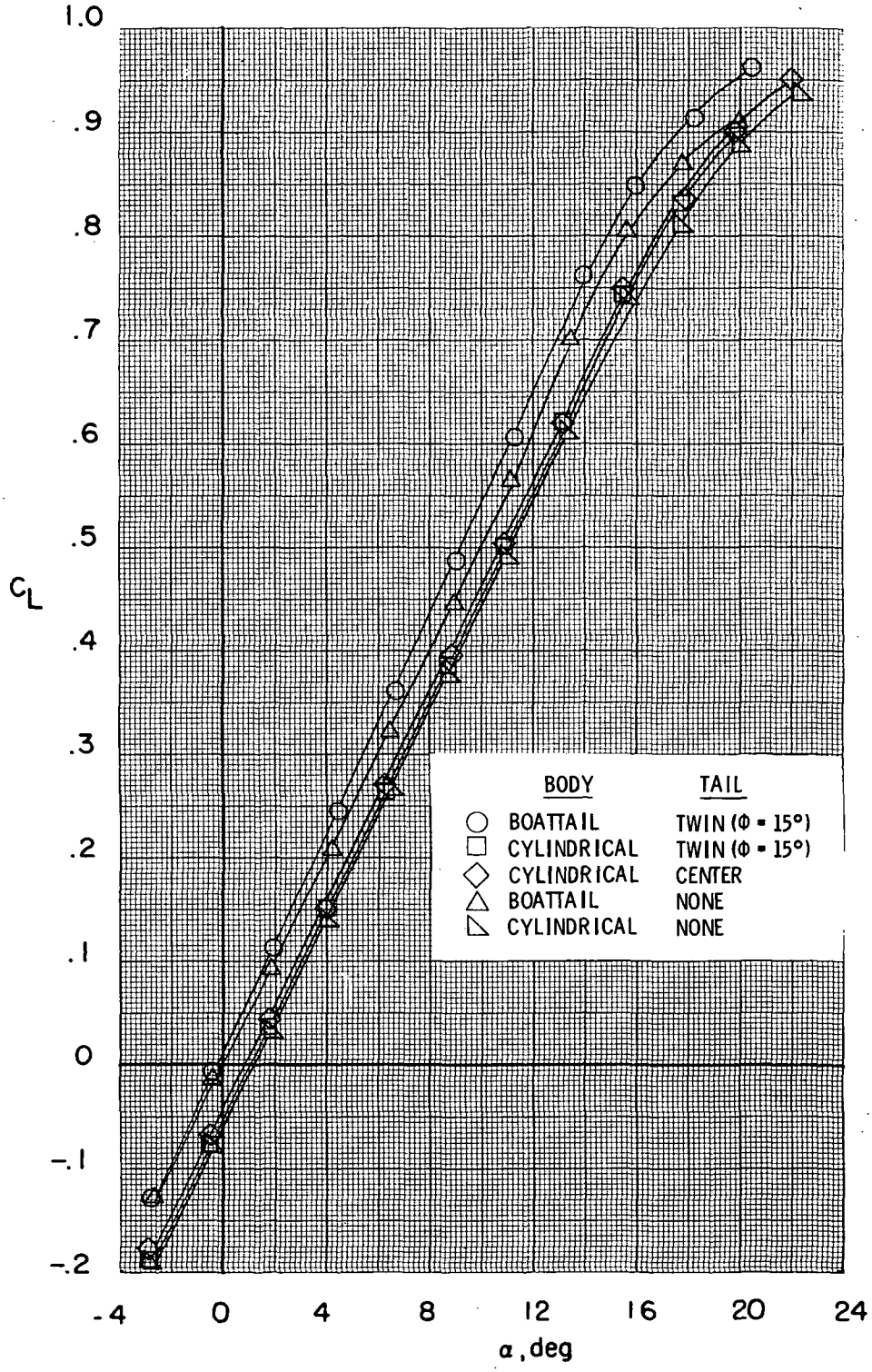

Figure 4.- Effect of configuration components on longitudinal aerodynamic characteristics of model. $\beta = 0^{o}$; $R = 13.9 \times 10^{6}$.

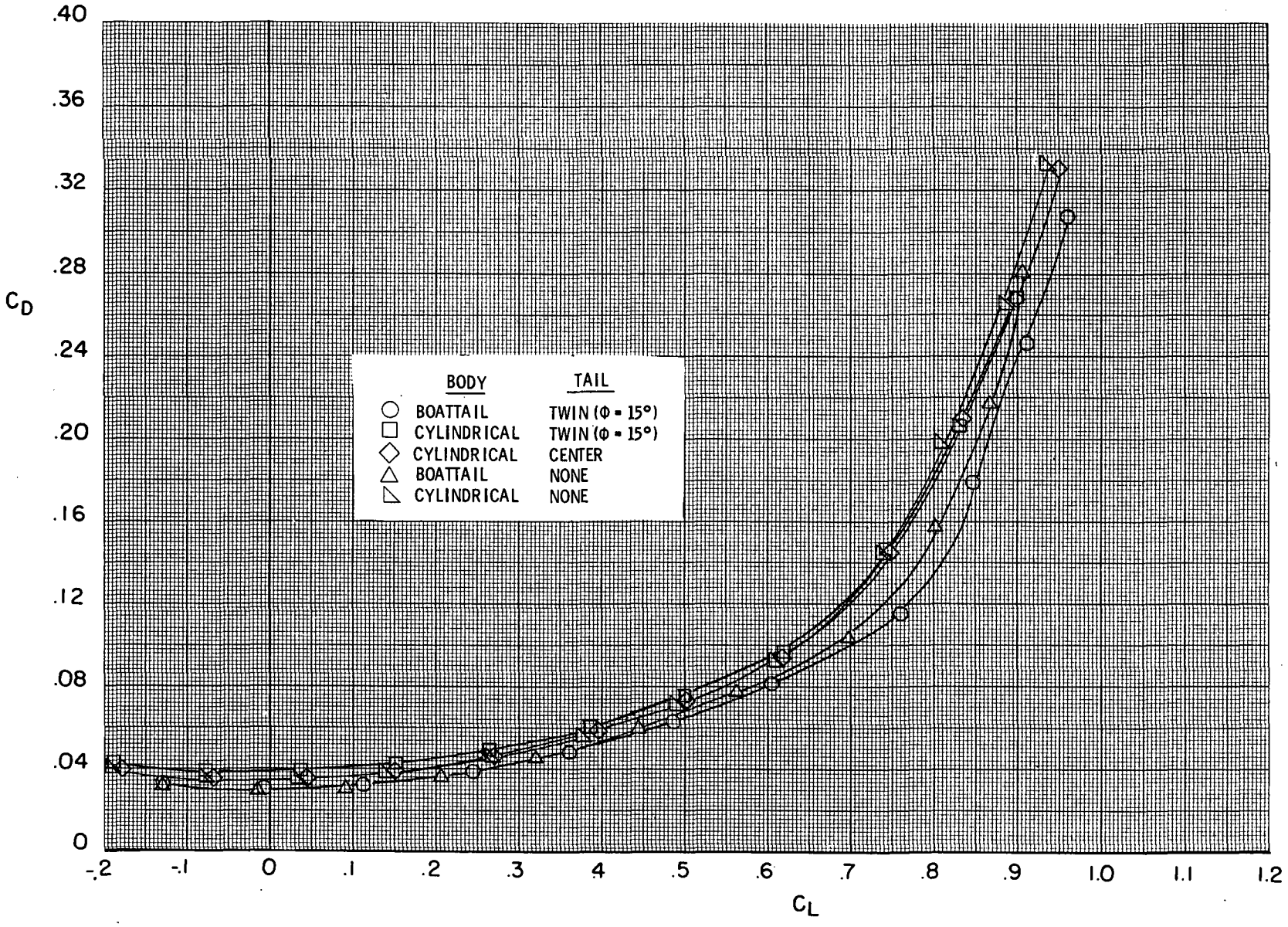

Figure 4.- Continued.

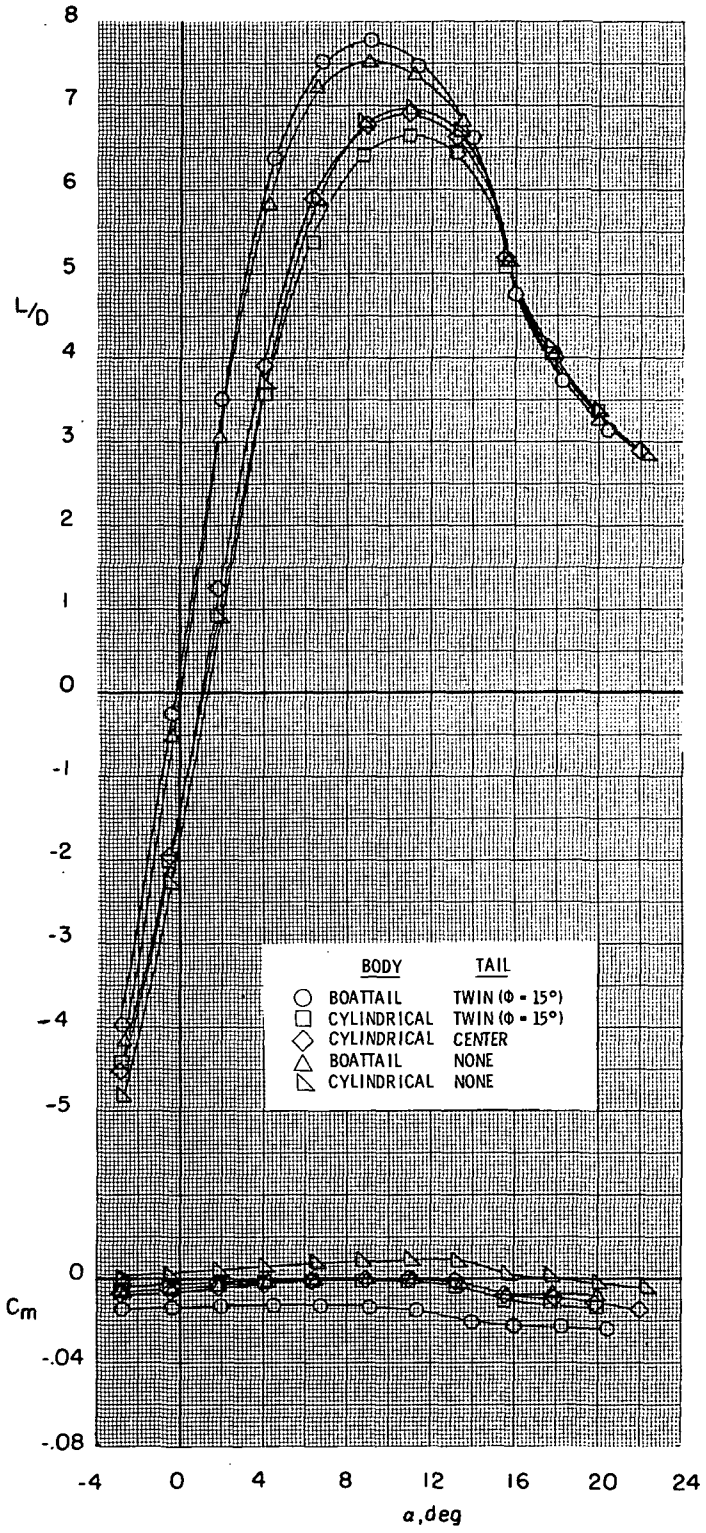

Figure 4.- Continued.

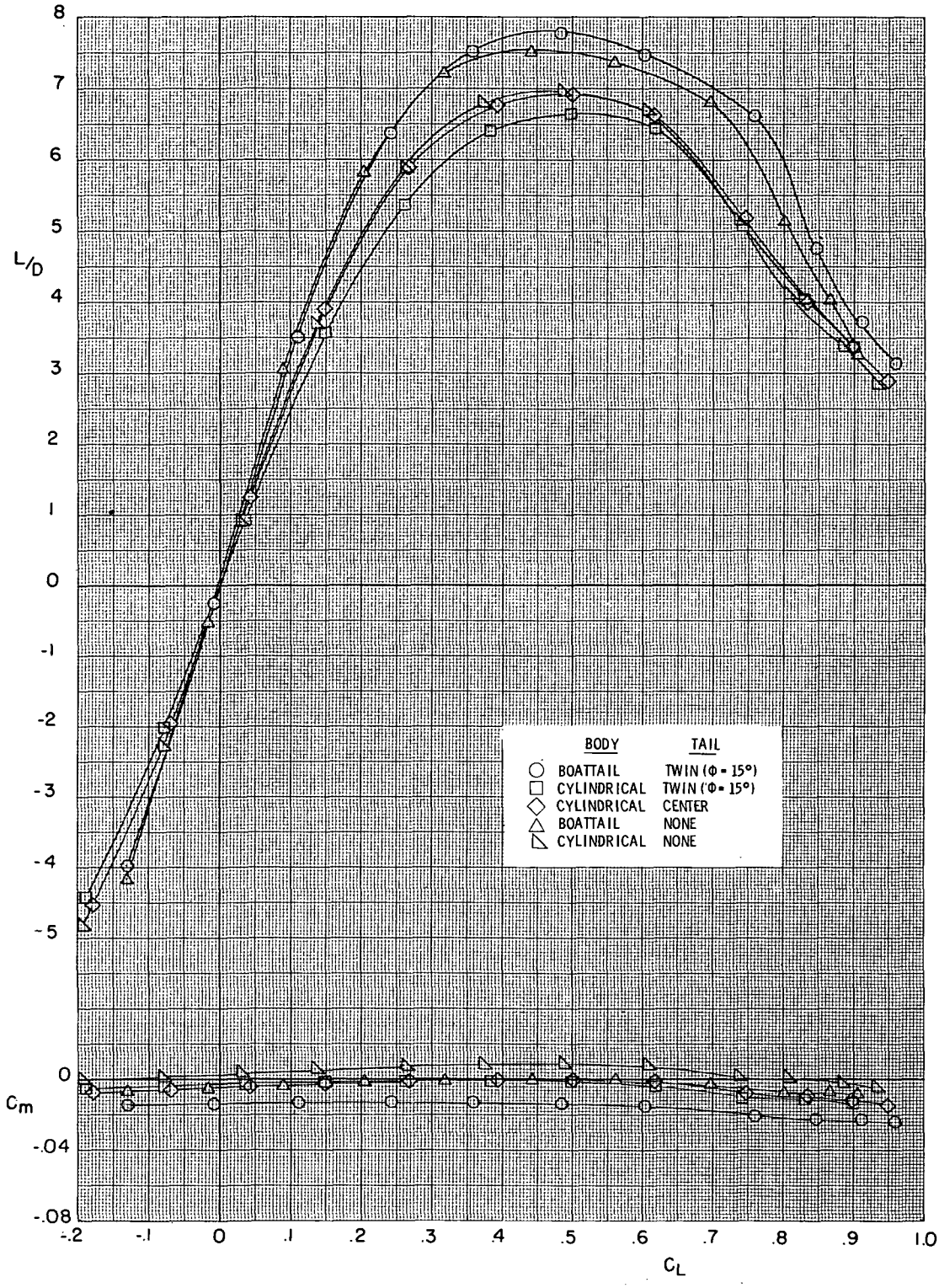

Figure 4.- Concluded.

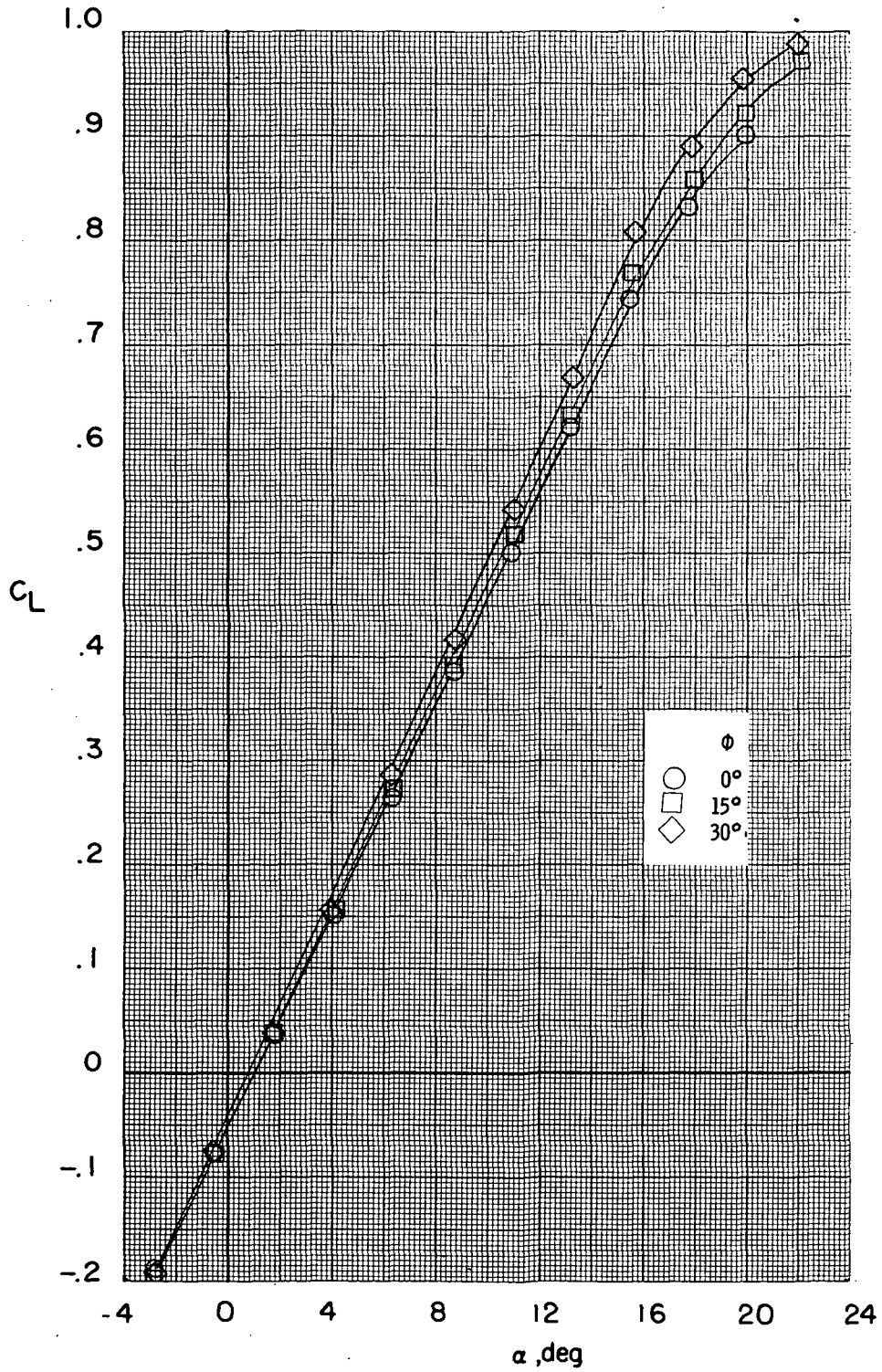

Figure 5.- Effect of twin tail roll-out angle on longitudinal aerodynamic characteristics of model. Cylindrical body; $\beta = 0^o$; $R = 13.9 \times 10^6$.

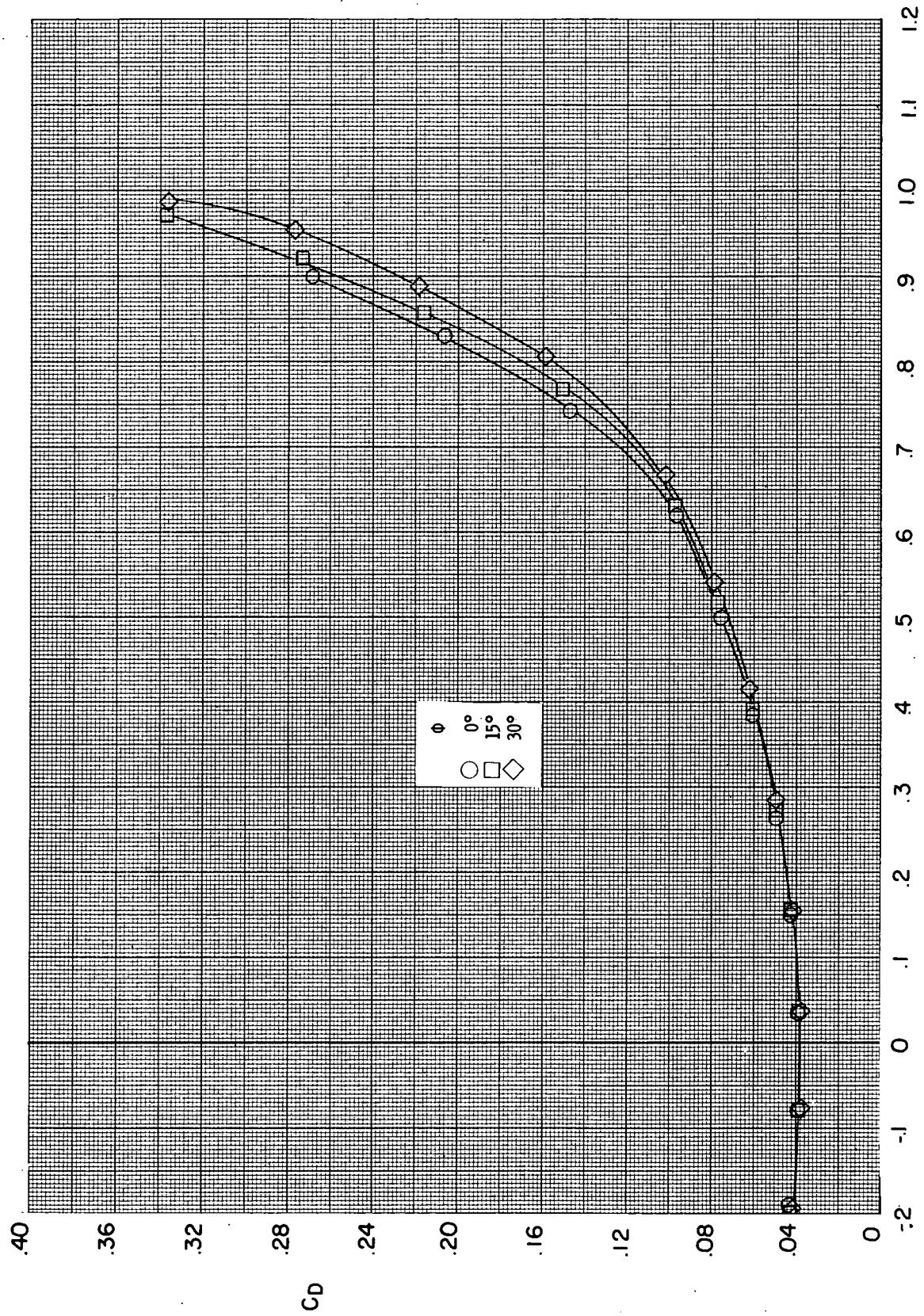

Figure 5.- Continued.

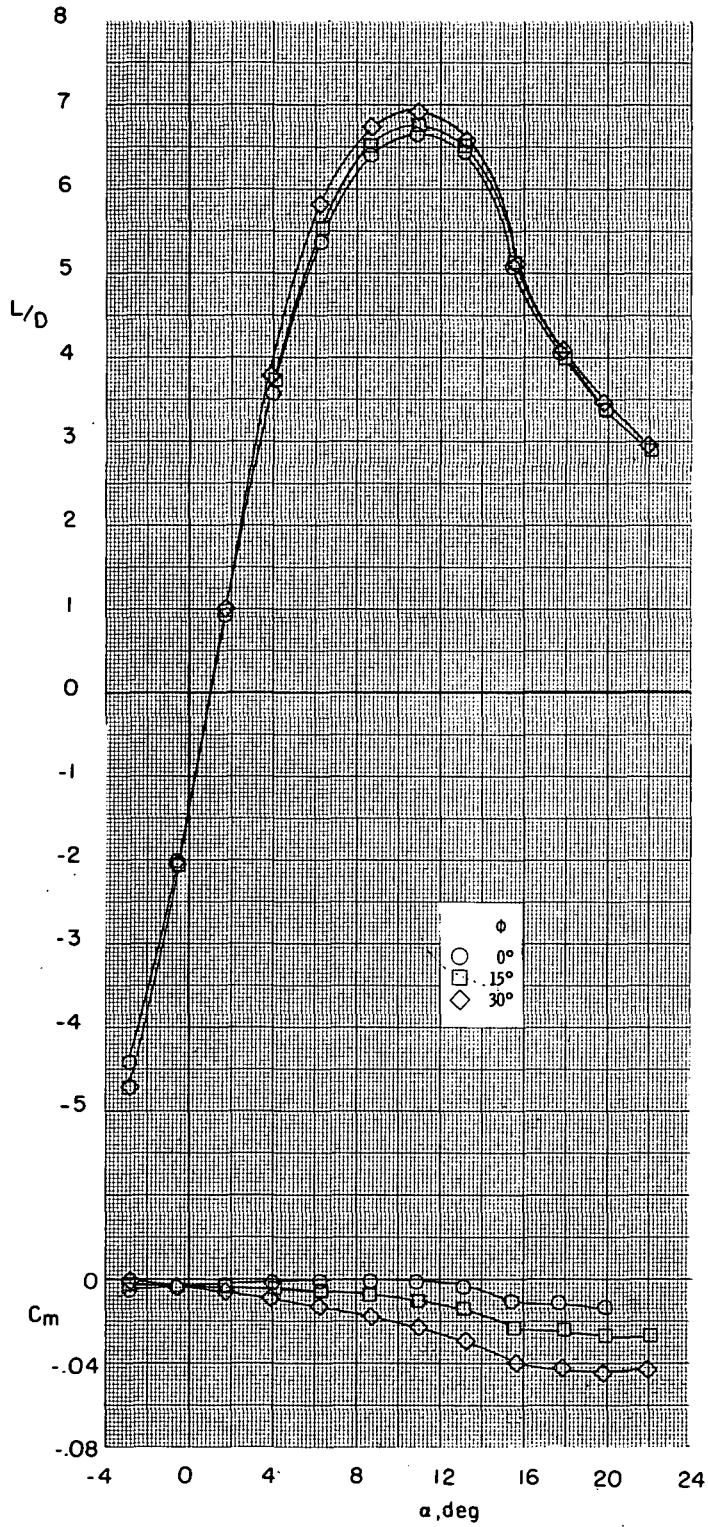

Figure 5.- Continued.

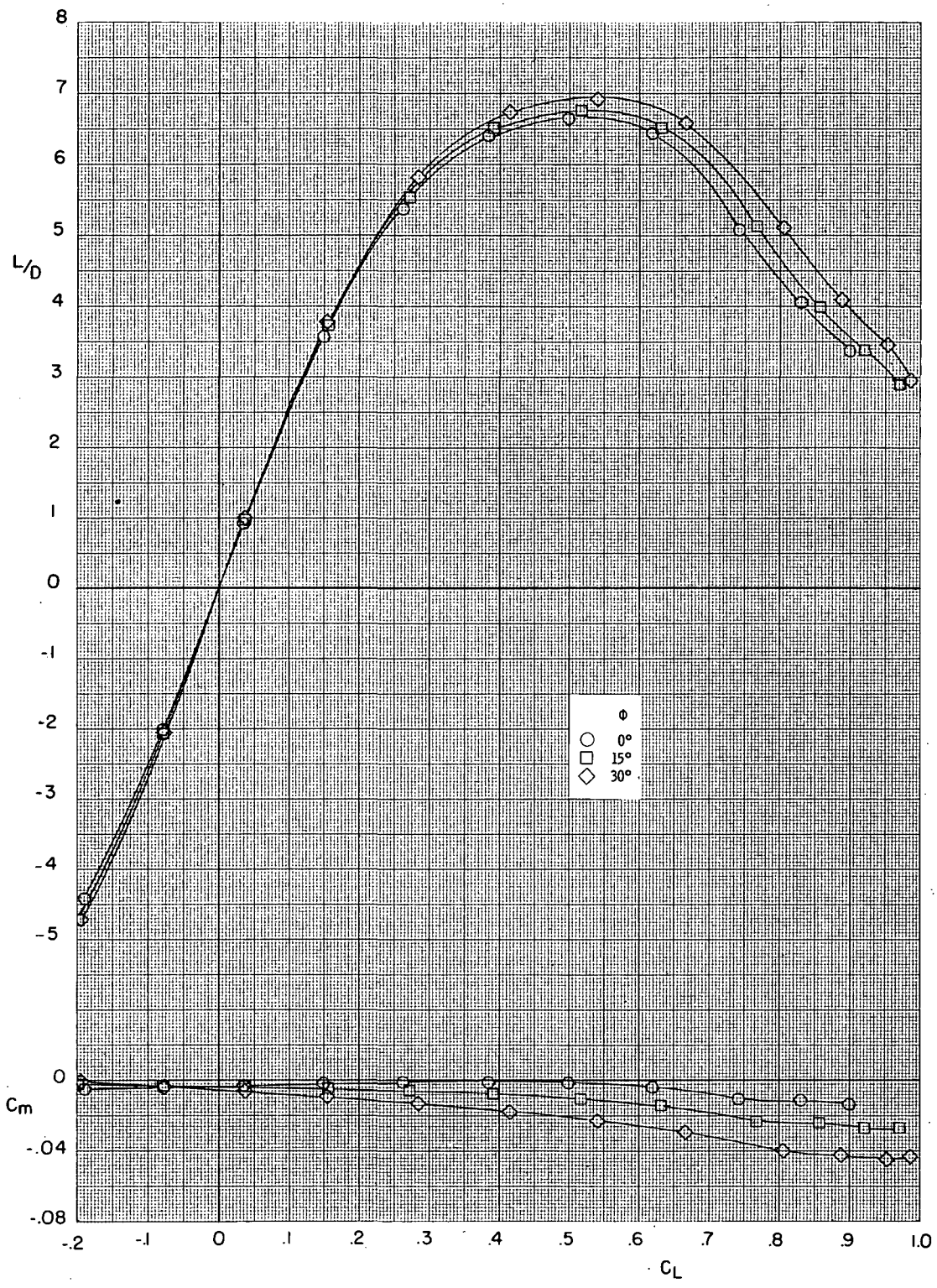

Figure 5.- Concluded.

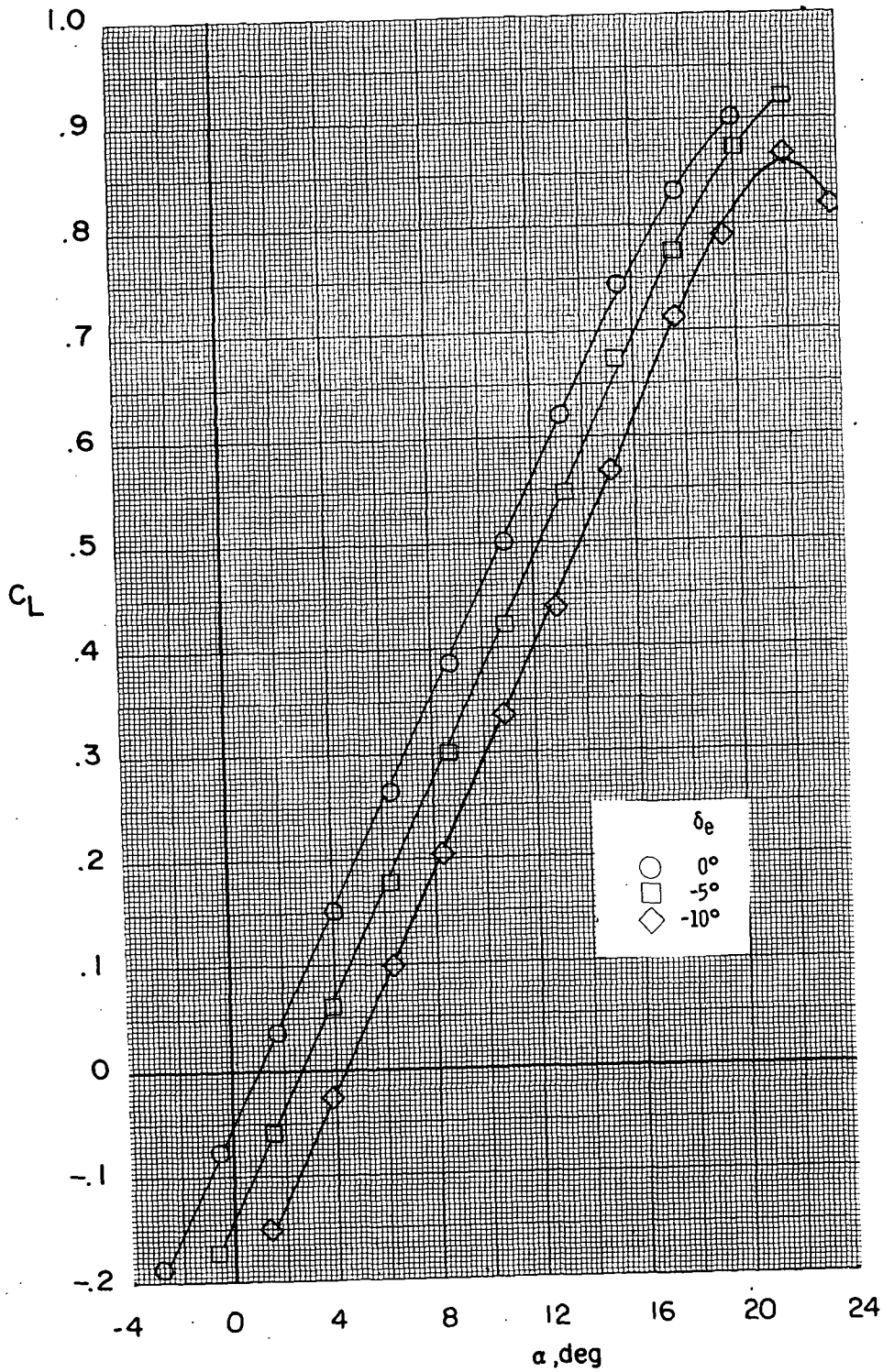

(a) Cylindrical body; twin tails ($\phi = 0^o$); $\beta = 0^o$; $R = 13.9 \times 10^6$.

Figure 6.- Effect of elevon deflection on longitudinal aerodynamic characteristics of model.

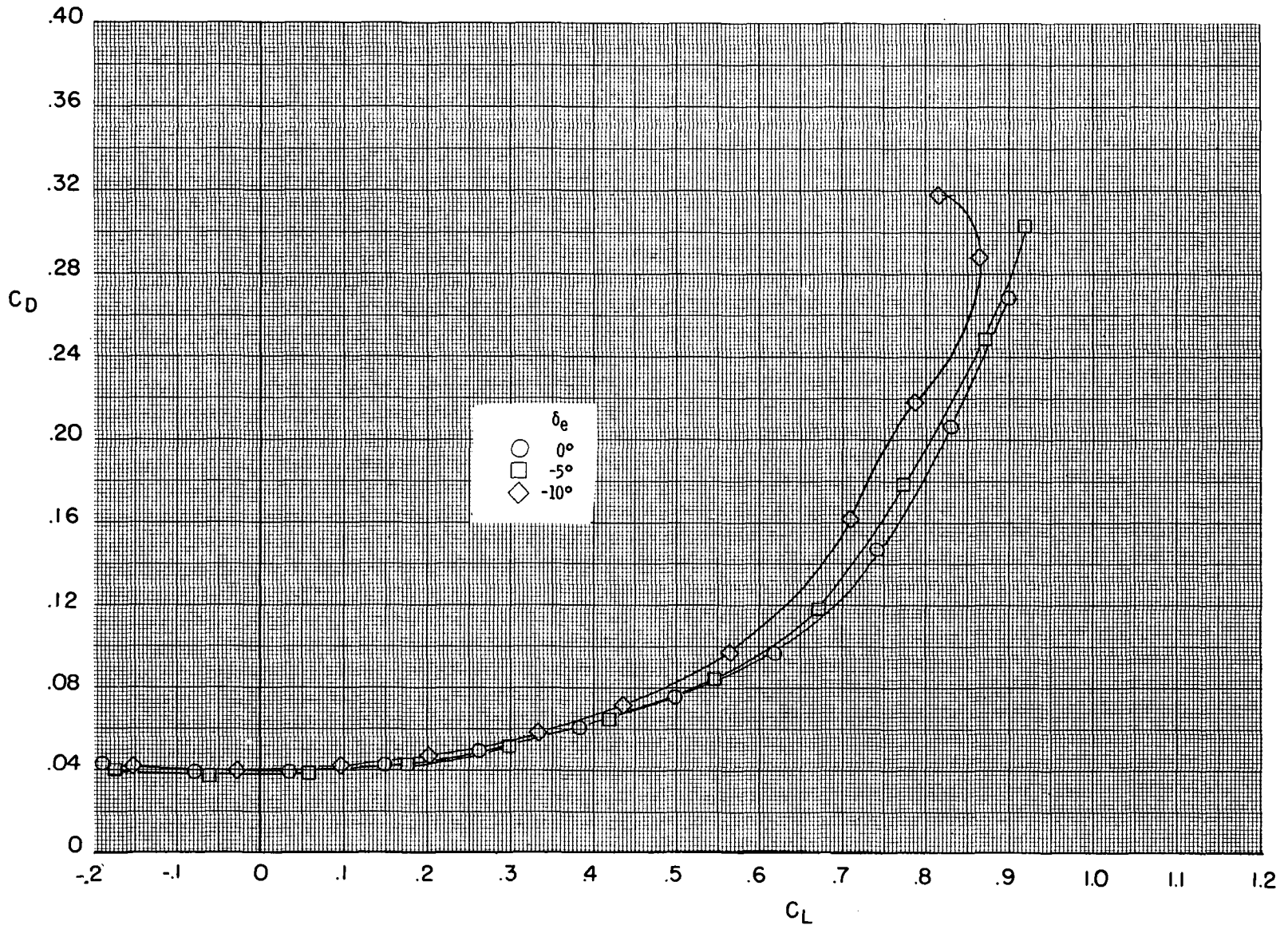

(a) Continued.

Figure 6.- Continued.

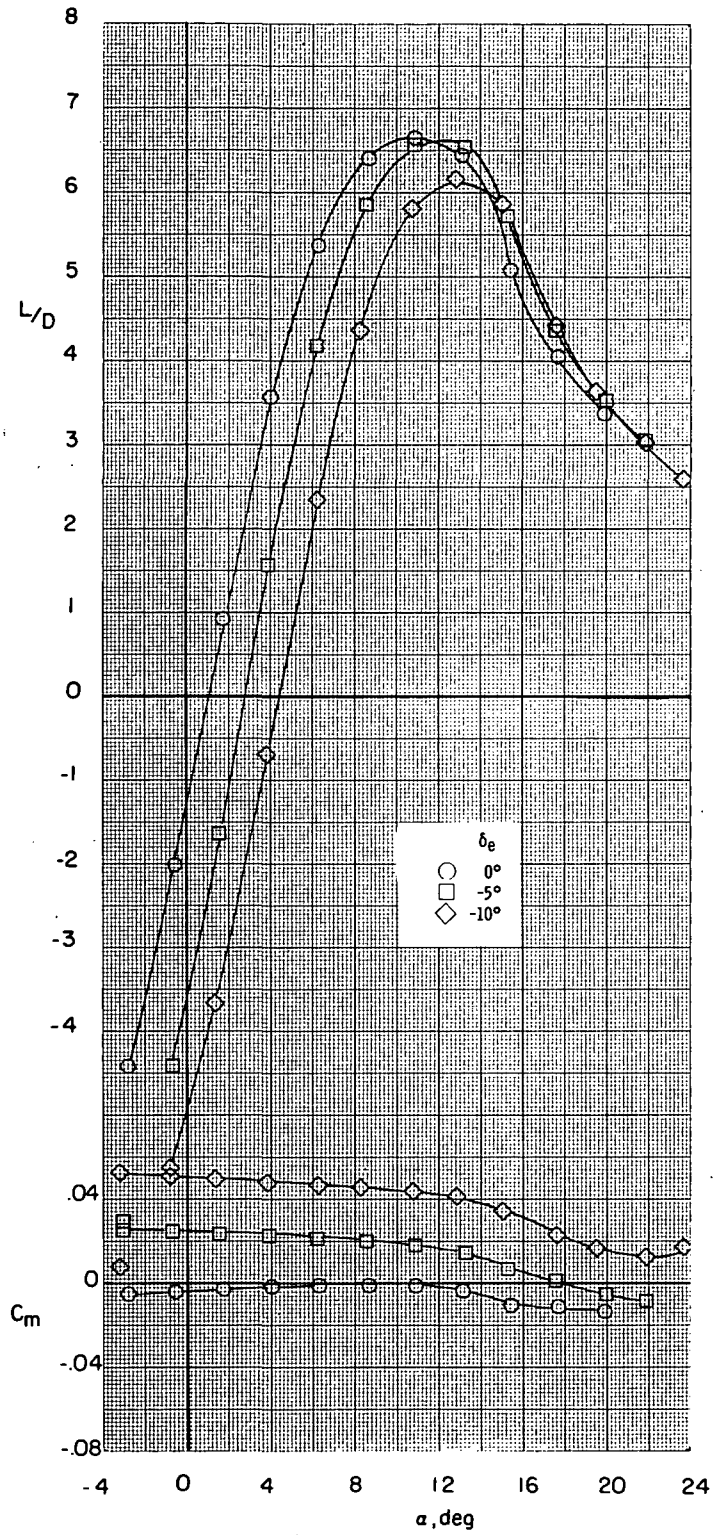

(a) Continued.

Figure 6.- Continued.

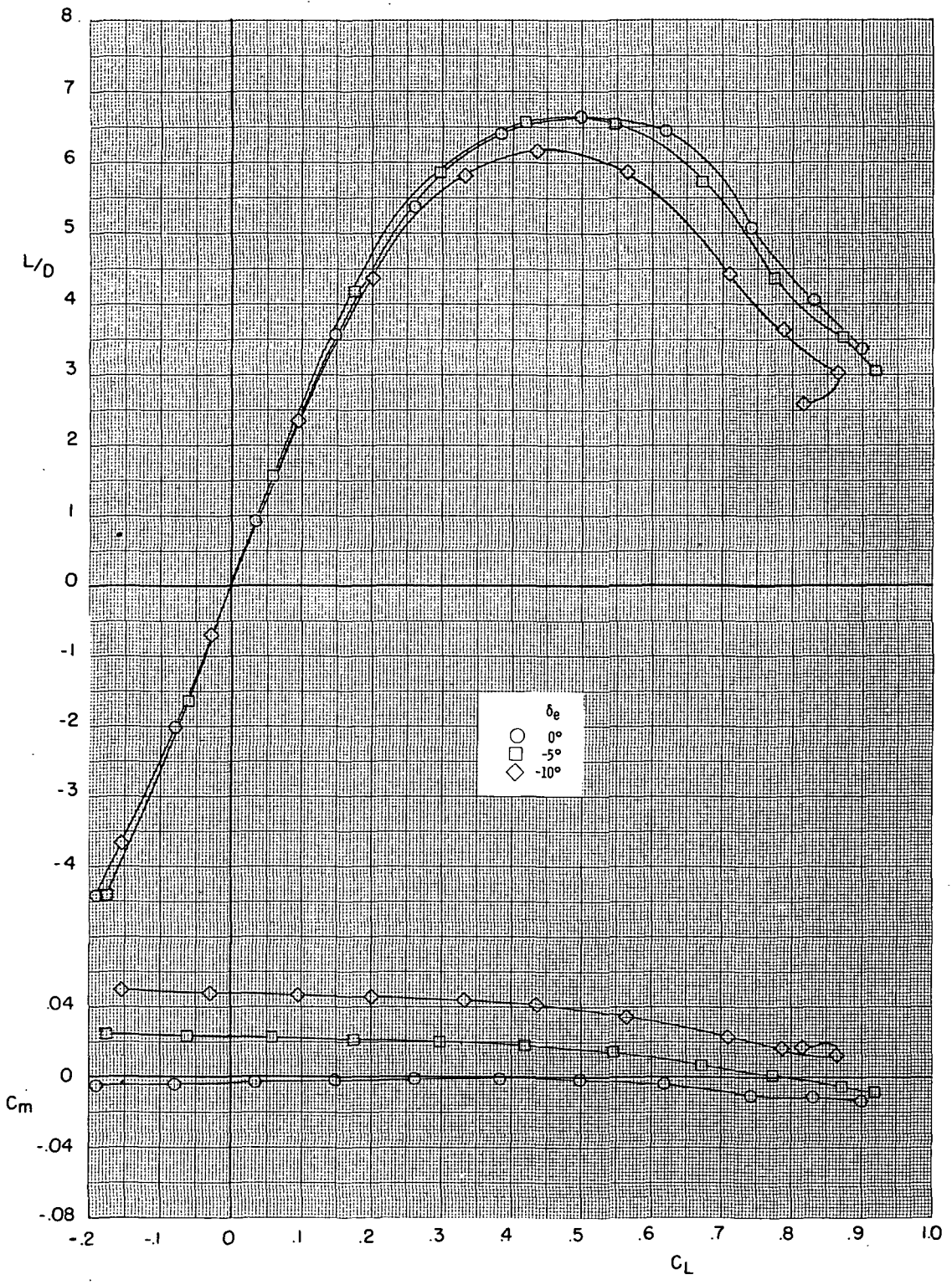

(a) Concluded.

Figure 6.- Continued.

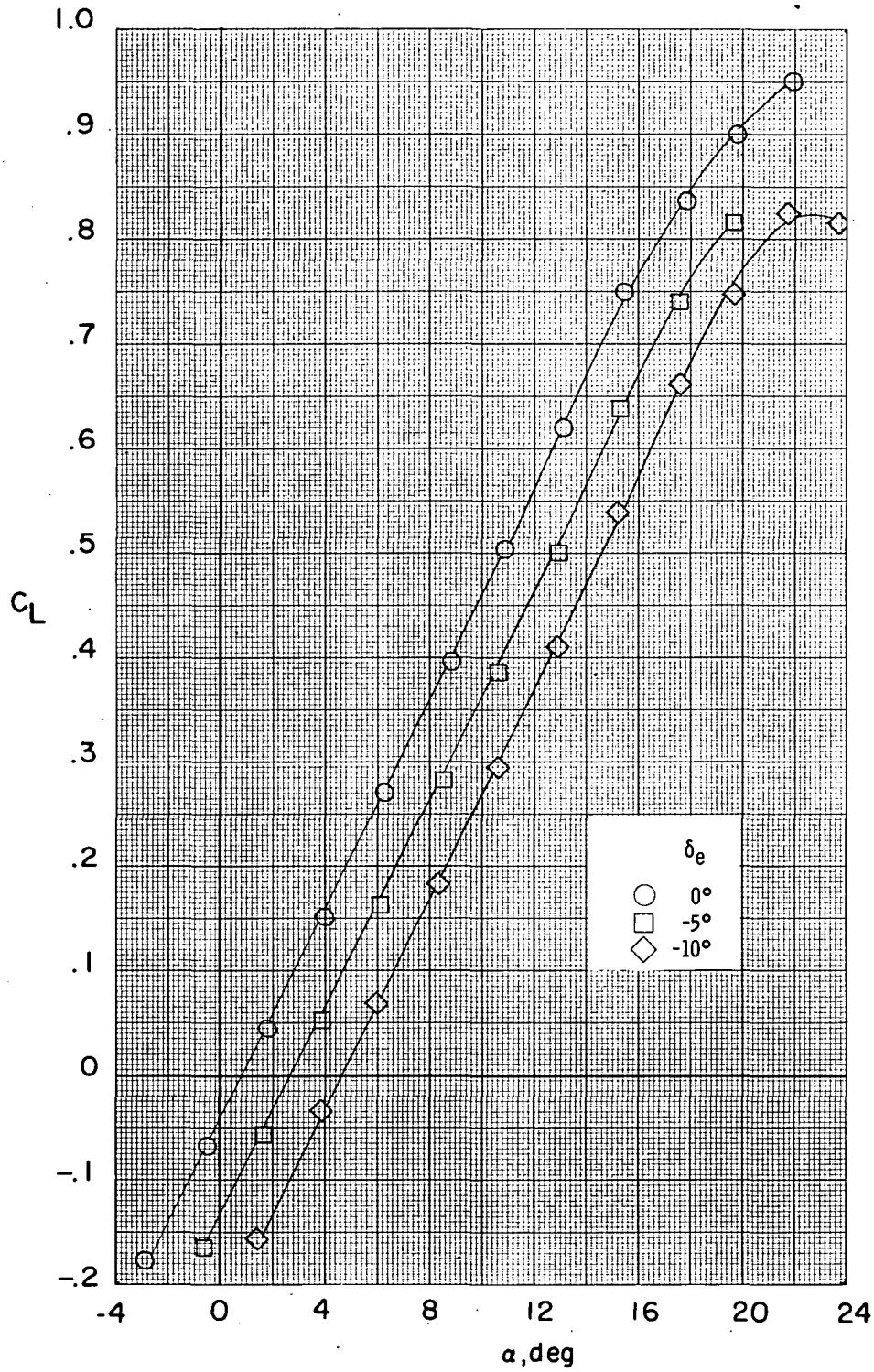

(b) Cylindrical body; center tail; $\beta = 0^o$; $R = 13.9 \times 10^6$.

Figure 6.- Continued.

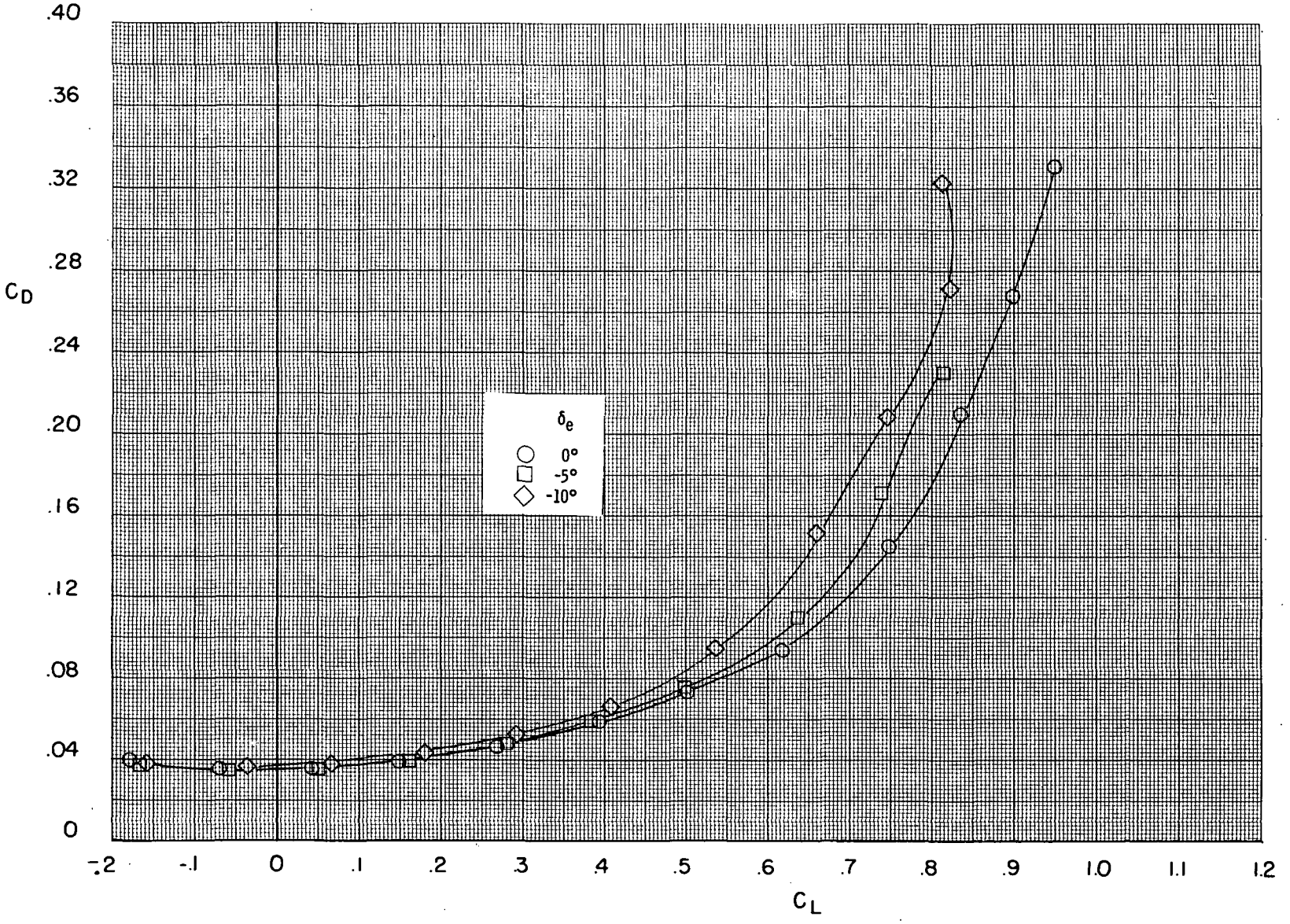

(b) Continued.

Figure 6.- Continued.

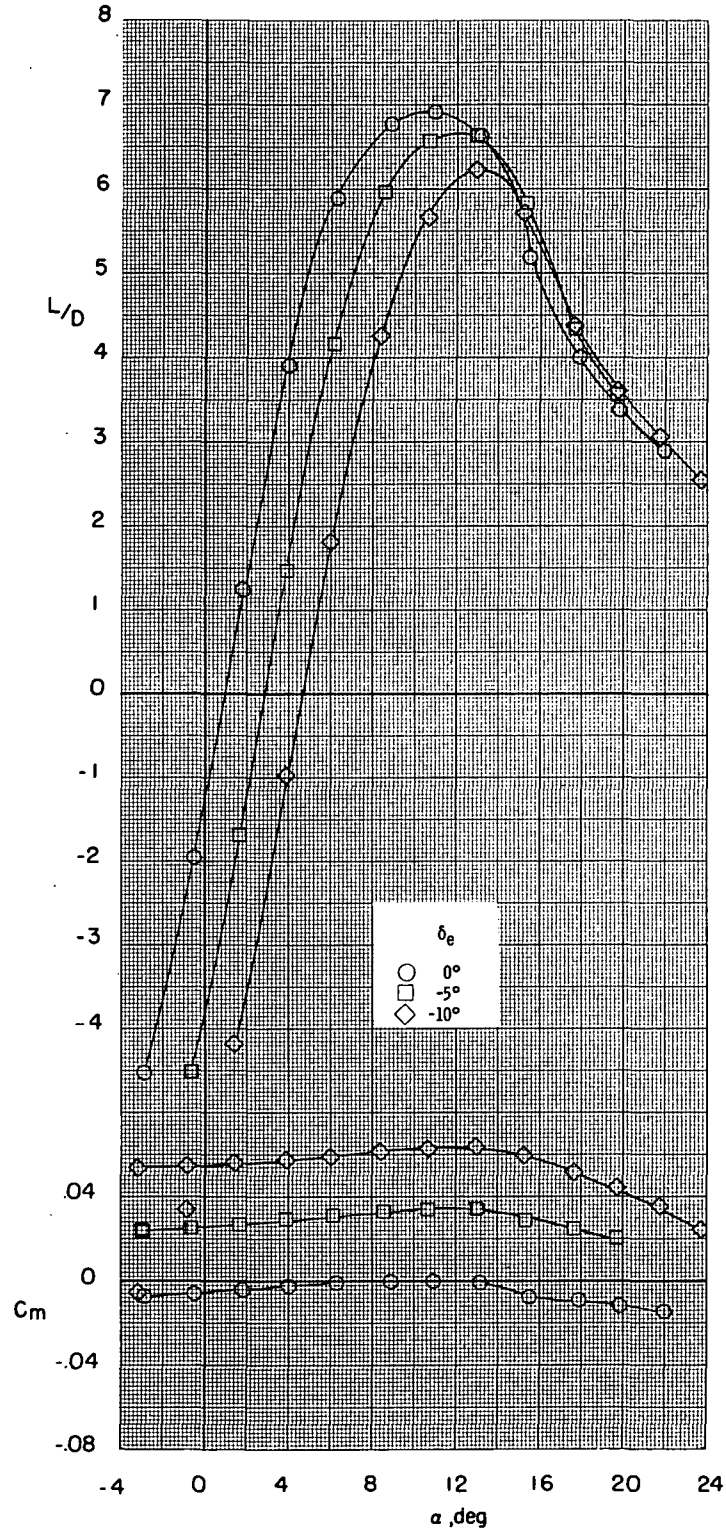

(b) Continued.

Figure 6.- Continued.

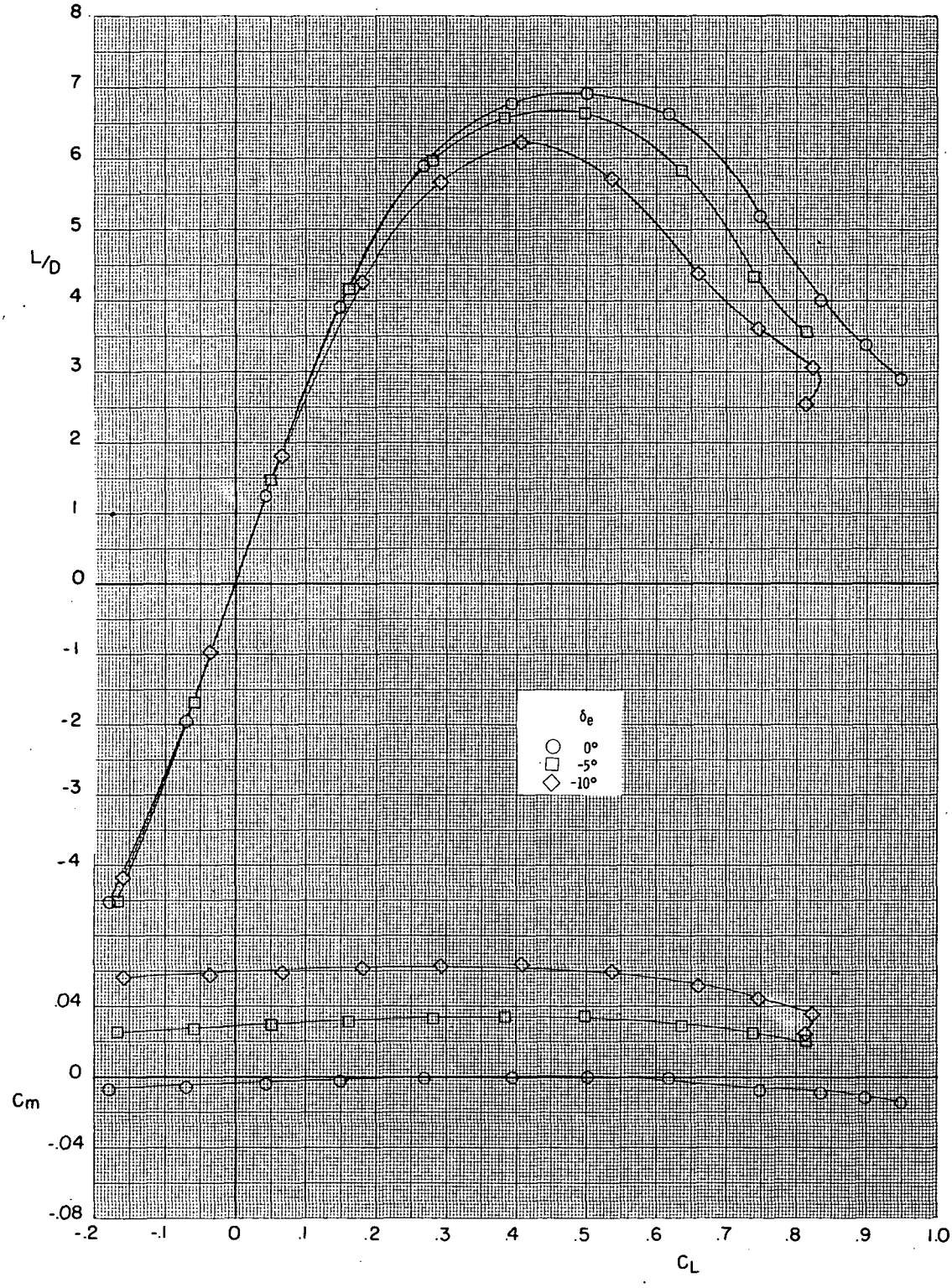

(b) Concluded.

Figure 6.- Concluded.

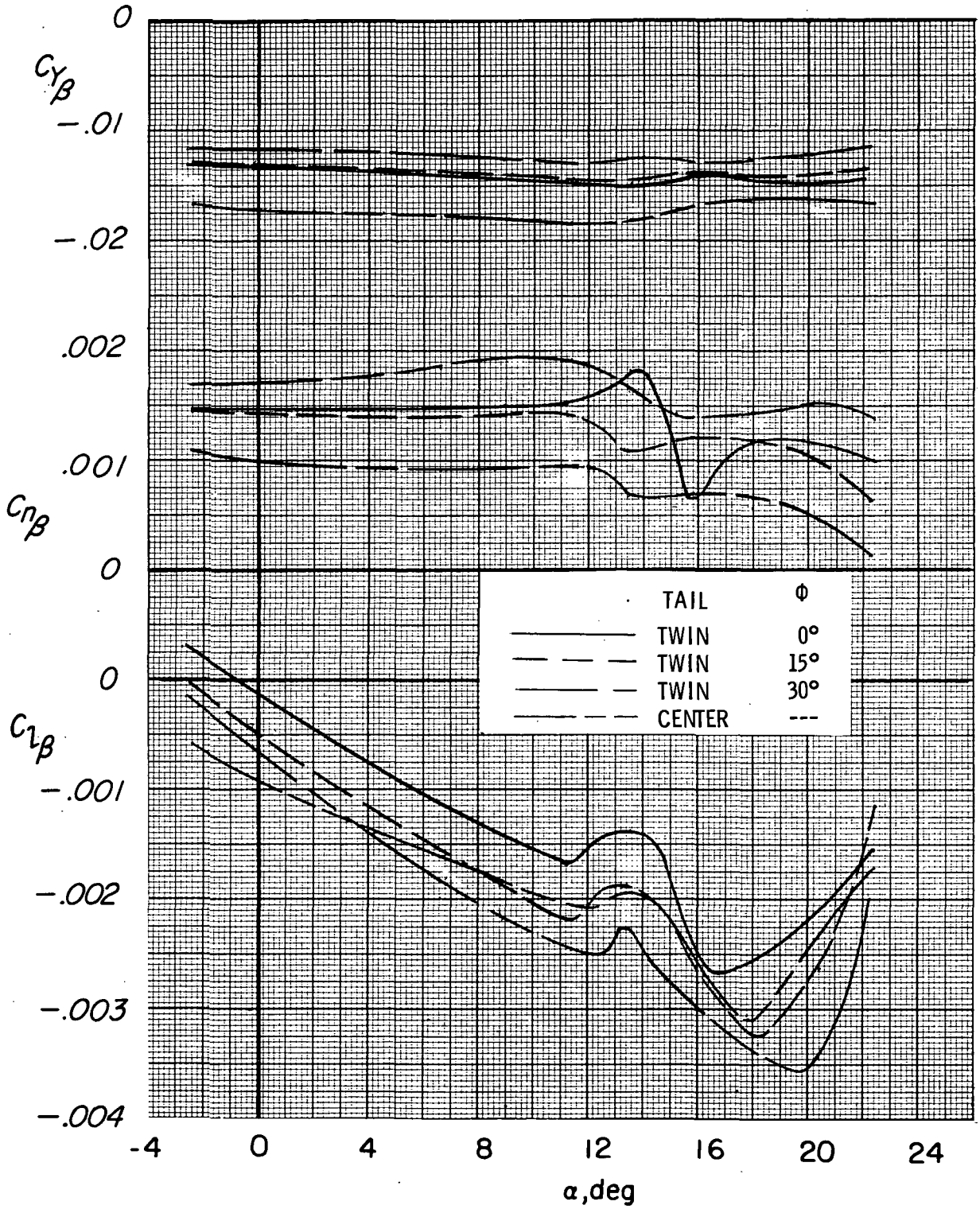

Figure 7.- Effect of vertical tail on lateral-directional characteristics of model. Cylindrical body; $R = 13.9 \times 10^6$.

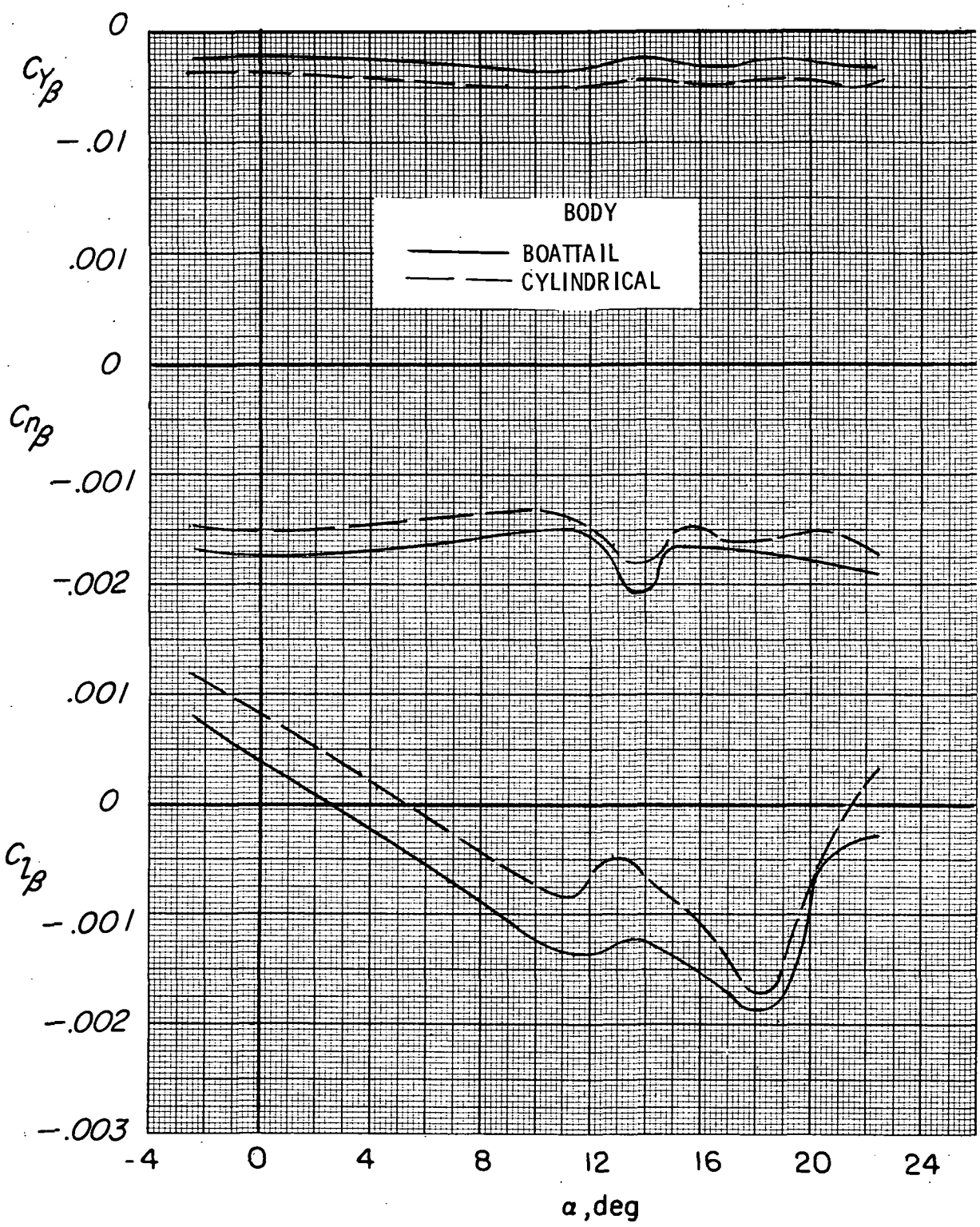

Figure 8.- Effect of boattail on lateral-directional characteristics of model. No vertical tails; $R = 13.9 \times 10^6$.

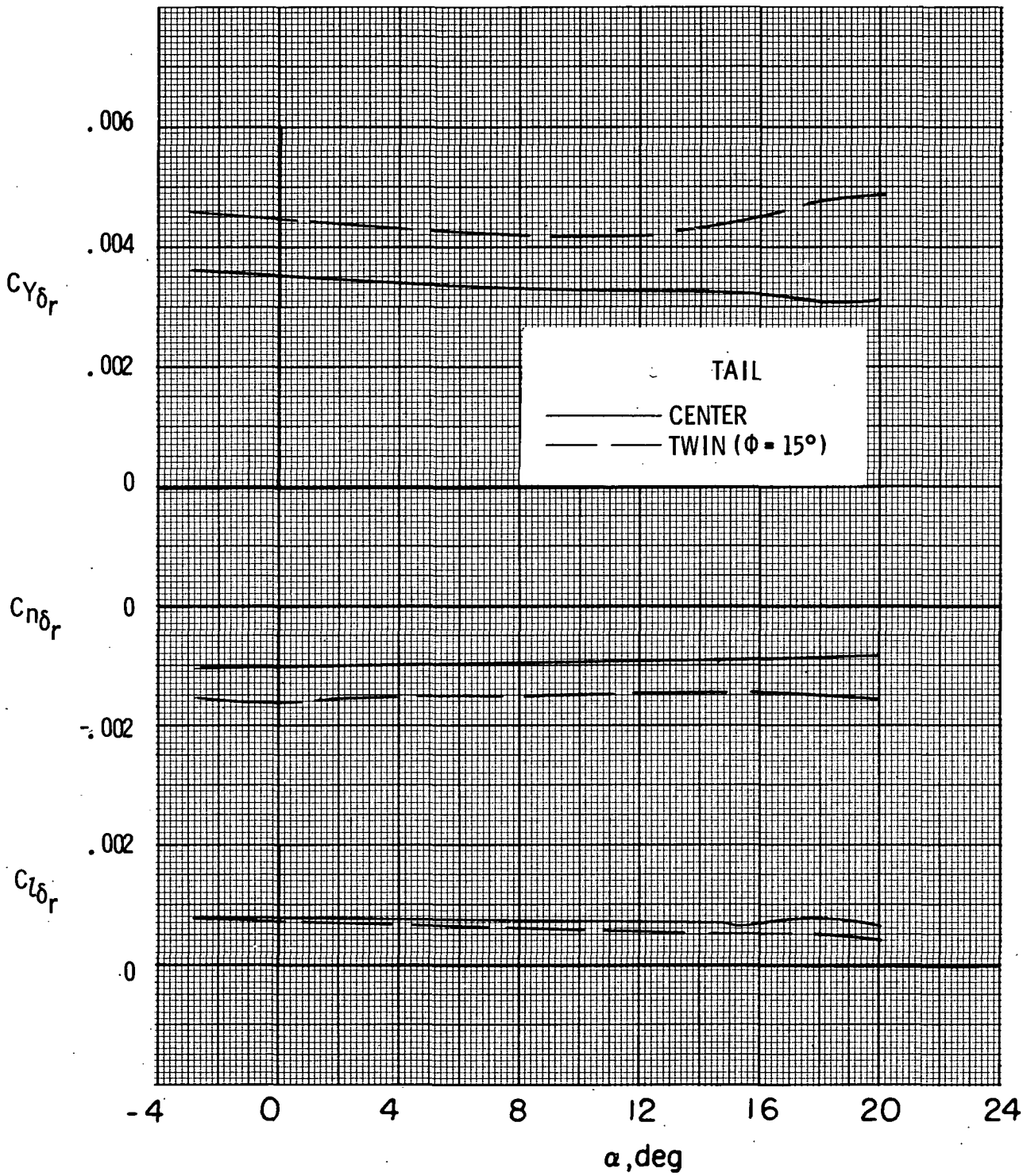

Figure 9.- Effect of rudder deflection as yaw control. Cylindrical body; $\delta_r = 10^o$; $R = 13.9 \times 10^6$.

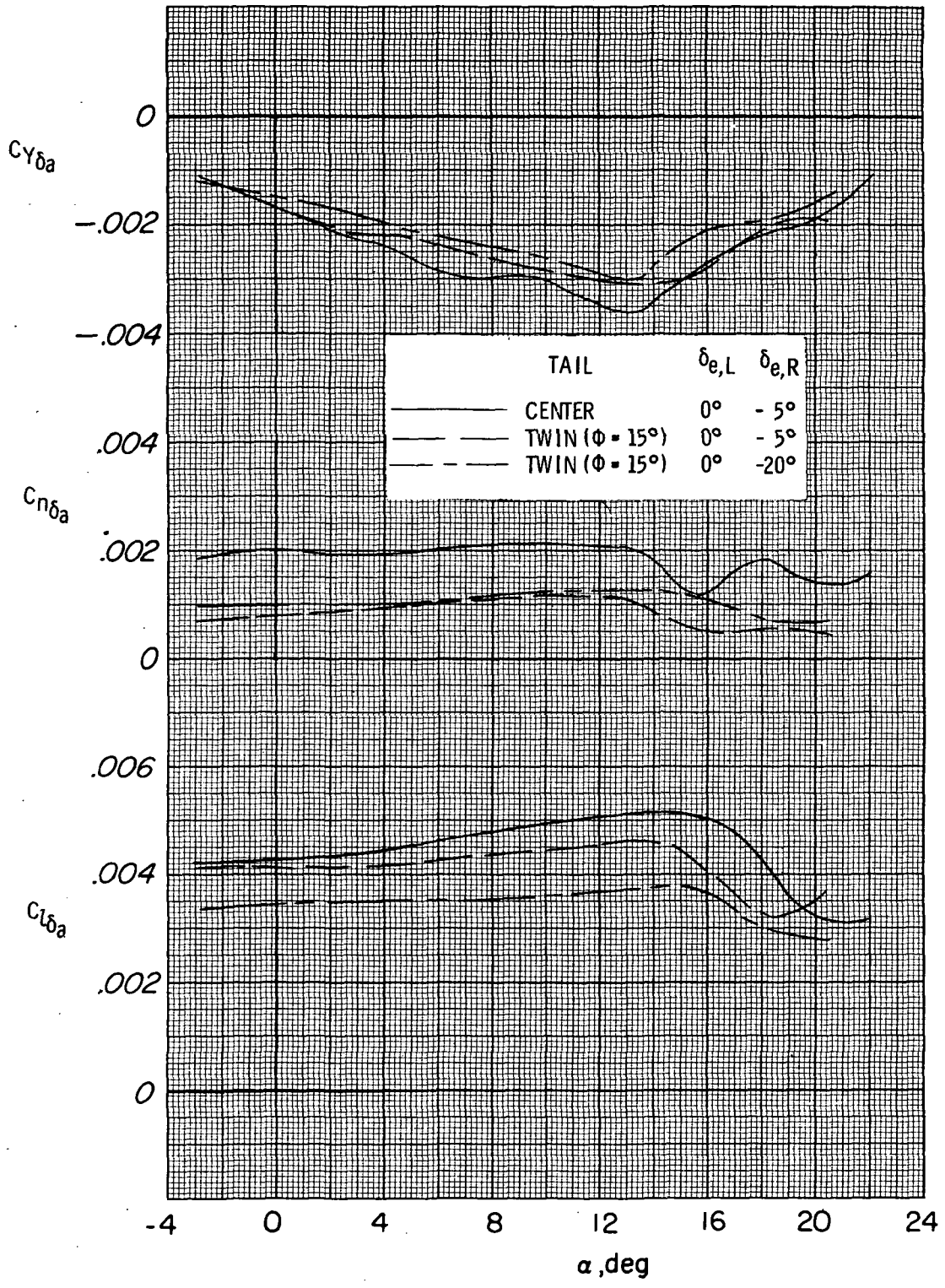

Figure 10.- Effect of aileron deflection as a roll control. Cylindrical body; $R = 13.9 \times 10^6$.

NASA-Langley, 1973 —— 1 L-8712

NATIONAL AERONAUTICS AND SPACE ADMINISTRATION
WASHINGTON, D.C. 20546

OFFICIAL BUSINESS
PENALTY FOR PRIVATE USE $300

SPECIAL FOURTH-CLASS RATE BOOK

POSTAGE AND FEES PAID
NATIONAL AERONAUTICS AND SPACE ADMINISTRATION
451

U.S.MAIL

POSTMASTER: If Undeliverable (Section 158 Postal Manual) Do Not Return

"The aeronautical and space activities of the United States shall be conducted so as to contribute . . . to the expansion of human knowledge of phenomena in the atmosphere and space. The Administration shall provide for the widest practicable and appropriate dissemination of information concerning its activities and the results thereof."

—NATIONAL AERONAUTICS AND SPACE ACT OF 1958

NASA SCIENTIFIC AND TECHNICAL PUBLICATIONS

TECHNICAL REPORTS: Scientific and technical information considered important, complete, and a lasting contribution to existing knowledge.

TECHNICAL NOTES: Information less broad in scope but nevertheless of importance as a contribution to existing knowledge.

TECHNICAL MEMORANDUMS: Information receiving limited distribution because of preliminary data, security classification, or other reasons. Also includes conference proceedings with either limited or unlimited distribution.

CONTRACTOR REPORTS: Scientific and technical information generated under a NASA contract or grant and considered an important contribution to existing knowledge.

TECHNICAL TRANSLATIONS: Information published in a foreign language considered to merit NASA distribution in English.

SPECIAL PUBLICATIONS: Information derived from or of value to NASA activities. Publications include final reports of major projects, monographs, data compilations, handbooks, sourcebooks, and special bibliographies.

TECHNOLOGY UTILIZATION PUBLICATIONS: Information on technology used by NASA that may be of particular interest in commercial and other non-aerospace applications. Publications include Tech Briefs, Technology Utilization Reports and Technology Surveys.

Details on the availability of these publications may be obtained from:

SCIENTIFIC AND TECHNICAL INFORMATION OFFICE

NATIONAL AERONAUTICS AND SPACE ADMINISTRATION

Washington, D.C. 20546